



UNIVERSITEIT VAN PRETORIA
UNIVERSITY OF PRETORIA
YUNIBESITHI YA PRETORIA

Denkleiers • Leading Minds • Dikgopolo tša Dihlalefi

New insights into the role of pH,
metal ions, and insoluble solids in
the co-production of fumarate and
malate by *Rhizopus delemar*

CVD 800

2022-07-07



UNIVERSITEIT VAN PRETORIA
UNIVERSITY OF PRETORIA
YUNIBESITHI YA PRETORIA
Denkleiers • Leading Minds • Dilkgopolo tša Dihlalefi

New insights into the role of pH, metal ions, and insoluble solids in the co-production of fumarate and malate by *Rhizopus delemar*

Dominic Kibet Ronoh
16278072

A thesis submitted in partial fulfilment of the requirements for the degree

Master of Engineering

in the

Department of Chemical Engineering
University of Pretoria

CVD 800

2022-07-07

New insights into the role of pH, metal ions, and insoluble solids in the co-production of fumarate and malate by *Rhizopus delemar*

Abstract

Calcium carbonate has been extensively used as a neutralising agent in acid forming microbial processes. The effect of increasing calcium carbonate concentrations on *Rhizopus delemar* has not been previously investigated. In this study, an evaluation of fumaric acid (FA) and malic acid (MA) production was conducted at three CaCO₃ concentrations in shake flask cultivations. Increased CaCO₃ concentrations resulted in the co-production of FA and MA in the first 55 h of the fermentation (regime 1), and the subsequent depletion of FA thereafter (regime 2).

Three factors were highlighted as likely causes of this response: insoluble solids, metal ion concentrations, and pH. Further shake flask cultivations as well as a continuous fermentation with immobilised *R. delemar* were used to explore the effect of the three factors on regime 1 and 2. Insoluble solids were found to have no effect on either the response in regime 1 or 2. Increasing the aqueous calcium ions concentrations to 10 g L⁻¹ resulted in a three-fold increase in MA titres (regime 1). Moreover, an increase in pH above 7 was associated with the drop in FA concentrations in regime 2. Further tests established that this was due to the hydration of FA to MA, influenced by high pH conditions (7 or higher), nitrogen starvation and glucose depletion. Anaerobic conditions were also found to significantly improve the hydration process.

This study presents the first investigation in which the production of FA followed by in situ hydration of FA to MA with *R. delemar* has been achieved.

Acknowledgments

My gratitude goes to MasterCard Foundation Scholarship Programme (University of Pretoria Chapter) for the continuous support over the years both financially and through various academic initiatives and mentorship programs that have helped shape the person that I have become. Though not directly involved in the research work, without them, neither this study nor my tertiary education would have been possible.

I would like to sincerely thank my supervisor, Prof. Hendrik Brink for ever being so gracious with his knowledge and time. His thoughtful stream of ideas helped fundamentally shape the direction of the research work, and for that I am grateful. I am also thankful to my co-supervisor, Prof. Willie Nicol for opening the doors to his bio-reaction engineering laboratories, and his willingness to assist without hesitation. I appreciate his bountiful wisdom and contagious energy, as well as his mentorship, guidance and dedication to my project and ensuring good quality work is achieved.

I personally wish to give thanks to the amazing team at the Bioreaction Engineering Research Group at the University of Pretoria. I could not have envisioned a better support system. Special thanks to Reuben Swart for his specific input into the research work.

My mother, Leah Ronoh and late father, Erick Ronoh are especially appreciated for their labour of love and prayers throughout this journey. I would not be here without them. To my family and friends who trod this path along with me, thank you.

Last but not least, I would like to thank God for His never ending mercies. All I can say is Ebenezer, *'Thus far the Lord has helped me'*.

Contents

Abstract	ii
1 Introduction	1
1.1 Outline of the dissertation	4
2 Literature review	5
2.1 The transition to a bio-based economy	5
2.1.1 Energy	5
2.1.2 Chemicals and materials	6
2.1.3 Transportation fuels	7
2.2 Microbial conversion of biomass into chemicals	8
2.2.1 Fumaric acid	9
2.2.2 Malic acid	10
2.3 Biocatalysts	12
2.3.1 <i>Rhizopus delemar</i>	12
2.3.2 Carbon metabolism	13
2.4 Neutralising agents	15
2.4.1 CaCO ₃	16
2.5 Future prospects	18
3 Experimental	19
3.1 Materials and methods	19
3.1.1 Microorganism	19

3.1.2	Inoculum preparation	19
3.1.3	Shake Flask Cultivations	19
3.1.4	Immobilised Reactor Cultivations	21
3.2	Sample Preparation	22
3.3	Analytical Methods	22
3.4	Mass Balance	24
4	Results and discussion	25
4.1	Biomass	25
4.2	Effect of CaCO ₃ addition	26
4.3	Effect of Insoluble Solids: Comparison with MgCO ₃	30
4.4	Effect of Insoluble Solids: Plaster Sand	33
4.5	Effect of calcium ions	36
4.6	Effect of pH	39
4.6.1	Glucose Steps	39
4.6.2	pH Steps	41
4.6.3	Hydration of FA to MA	42
5	Conclusion and recommendations	47

List of Figures

1	Global primary energy consumption by source	5
2	Energy Consumption by Sector, OECD Countries	7
3	Transportation energy sources, 2020	8
4	Fumaric acid structure	10
5	Metabolic pathways of <i>Rhizopus delemar</i>	15
6	Morphology of fungal biomass: (a) pellets (b) biofilm	25
7	Shake flask cultivations with increasing concentrations of CaCO_3	27
8	Metabolite distribution of <i>Rhizopus delemar</i> with the minor components including biomass, succinic acid and pyruvic acid.	29
9	Shake flask cultivations with increasing concentrations of MgCO_3	32
10	<i>R. delemar</i> pellets at the end of the plaster sand run. The pellets were collected from the flask that contained 20 g L^{-1} CaCO_3 for pH control and 120 g L^{-1} plaster sand	34
11	The effect of increased concentrations of insoluble solids on fumarate and malate production	36
12	The effect of increased concentrations of calcium ions on fumarate and malate production	38
13	Glucose dosing rates and extracellular concentrations of (a)fumaric acid, (b) malic acid, (c)ethanol, and (d) glucose	40
14	pH steps, and extracellular concentrations of (a) fumarate, (b) malate and ethanol	42
15	pH steps, and extracellular concentrations of (a) fumarate, malate and (b) side products	44
16	Extracellular concentrations of glycerol during shake flask cultivation of <i>R. delemar</i> with different plaster sand concentrations. Results are the mean of triplicate experiments and error bars indicate the standard deviation.	60

17 Extracellular concentrations of glycerol during shake flask cultivation of *R. delemar* with different calcium ion concentrations. 20 g L⁻¹ CaCO₃ was used for pH control as a baseline amount in these experiments and additional 5, 10 and 20 g L⁻¹ calcium ions were added onto the baseline in the form of CaCl₂. 60

List of Tables

1	Fumaric acid production studies with <i>R. delemar</i> using different neutralising agents	17
2	HPLC standard calibration: Concentration and coefficient of determination (R^2) values for Glucose, malate, fumarate, glycerol, and ethanol . . .	23
3	Inductively coupled plasma (ICP) measurements of Ca^{2+} and Mg^{2+} at the end of each fermentation condition (198h) in comparison to the baseline amount	31
4	Comparison of fumaric acid and malic acid production using <i>R. delemar</i> .	45

List of nomenclature

Ac-CoA	Acetyl coenzyme A
ATCC	American Type Culture Collection
ATP	Adenosine triphosphate
C_x	Concentration of components (g L^{-1})
$\Delta G_0'$	Gibbs free energy (kJ mol^{-1})
DOE	Department of Energy
DOR	Degree of Reduction
EIA	Energy Information Administration
FA	Fumaric acid
FDA	Food and Drug Administration
FADH ₂	Flavin adenine dinucleotide
FUM	Fumarase
GTP	Guanosine-5-triphosphate
GHG	Greenhouse gas
GRAS	Generally regarded as safe
HPLC	High performance liquid chromatography
ICP	Inductively coupled plasma
IEA	International Energy Agency
MA	Malic acid
MDH	Malate dehydrogenase
NADH	Nicotinamide adenine dinucleotide
OES	Optical emission spectrometry

PDA	Potato dextrose agar
PMA	Polymalic acid
PS	Plaster sand
PYC	Pyruvate carboxylase
RBC	Rotary biofilm contractor
RPM	Revolutions per minute
TCA	Tricarboxylic acid

Research outputs

1. Ronoh, D.K.; Swart, R.M.; Nicol, W.; Brink, H. The Effect of pH, Metal Ions, and Insoluble Solids on the Production of Fumarate and Malate by *Rhizopus delemar* in the Presence of CaCO₃. *Catalysts* **2022**, 12, 263. <https://doi.org/10.3390/catal12030263>
2. Swart, R.M.; Ronoh, D.K.; Brink, H.; Nicol, W. Continuous Production of Fumaric Acid with Immobilised *Rhizopus oryzae*: The Role of pH and Urea Addition. *Catalysts* **2022**, 12, 82. <https://doi.org/10.3390/catal12010082>

1 Introduction

The rate at which fossil resources are depleting, coupled with the resultant deterioration of the global environment has been a major source of concern in the past few decades (Meussen *et al*, 2012; Martin-Dominguez, Bouzas-Santiso, *et al*, 2020). As a result, many research efforts have been focused on the development of alternative sources of feedstock to replace fossil resources. Wind, nuclear, solar and geothermal energy are only but a few of the energy generation alternatives currently available. However, biomass derived products are the only practicable alternatives for the generation of transportation fuels and platform chemicals (Meussen *et al*, 2012; Sebastian *et al*, 2019). In 2004, the Department of Energy (DOE) identified 12 chemical building blocks obtainable from biomass as potential platform chemicals (Werpy & Petersen, 2004).

Fermentative methods with the aid of microorganisms to produce organic acids were partially developed in the 1940s but were quickly abandoned due to the more lucrative chemical methods developed after World War II (G Xu *et al*, 2013; Goldberg, Rokem & Pines, 2006; Z Zhou *et al*, 2011; Li *et al*, 2016). However recent renewed interest has led many researchers to focus on the development and optimisation of these fermentative methods (Huang *et al*, 2010; Roa Engel, Straathof, *et al*, 2008). The microorganisms used in the bioproduction of organic acids must exhibit high yields, productivities and titres in order to compete with processes based on petrochemical methods. Other prerequisites for their economic feasibility include the ability to use many different carbon sources, ability to grow in the absence of complex growth factors, and resistance to fermentation inhibitors (Roa Engel, Straathof, *et al*, 2008; Meussen *et al*, 2012).

Rhizopus oryzae is a prominent zygomycetes fungus, well known for its ability to sustainably produce platform chemicals such as lactic acid (Type I strain) and fumaric and malic acids (Type II strain). The latter is correctly referred to as *Rhizopus delemar*, although the name has not been commonly adapted in literature (Sebastian *et al*, 2019; Abe, Oda, *et al*, 2007). *R. delemar* will be used henceforth in this research for clarity purposes. Compared against the metric above, *R. delemar* is the most successful fumaric acid producer, with the highest yield reported as 0.93 g g^{-1} in homofumarate production using immobilised fungus (Swart, Ronoh, *et al*, 2022). Additionally, significantly high productivities have been reported from immobilised *R. delemar* with a rotary biofilm contactor and an adsorption column (Cao *et al*, 1996). *R. delemar* has also been flagged for its ability to grow on a wide range of carbon sources, including glycerol, ethanol, lactic acid, glucose, mannose, sucrose and other fermentable sugars (Meussen *et al*, 2012; Skory, 2004; Sebastian *et al*, 2019). Moreover, its well demonstrated growth ability in a wide array of unspecific and inexpensive culture media, along with its ability to survive in a

wide temperature and pH range (up to 40 °C and 4-9, respectively) positions *R. delemar* mediated fermentations well as a worthy and competitive alternative to petrochemical methods (Ferreira *et al*, 2013; Meussen *et al*, 2012).

However, since many *Rhizopus* species spend at least a portion of their life cycle as free living organisms, they are exquisitely sensitive to changes in their environment (Machtelt *et al*, 2005). Such sensing and integration of signals from multiple sources (abiotic and biotic) result in the main challenge faced in *R. delemar* mediated fermentations; pH sensitivity, resulting in a need for continuous neutralisation (Gangl, Weigand & Keller, 1990). Consequentially, research efforts have focused on exploring the effect of different neutralising agents on fumaric acid yields and titres, determining the optimum pH conditions, and developing low pH fermentation strategies to bypass the need to use neutralising agents (Zhou, Du & Tsao, 2002; Gangl *et al*, 1990; Swart, Le Roux, *et al*, 2020; Y Liu *et al*, 2015; Roa Engel, Van Gulik, *et al*, 2011).

Among the neutralising agents commonly used especially in applications without online pH monitoring and control is CaCO₃, a naturally occurring chemical compound favoured due to its abundance, poor solubility, and relatively low cost (Salek *et al*, 2015). In fact, nearly all previous investigators of fumaric and malic acid production by *Rhizopus* species that have used the base calcium carbonate have indicated significantly higher yields, titres, and productivities in comparison to other neutralising agents such as calcium hydroxide, sodium carbonate, sodium bicarbonate, and sodium hydroxide (Gangl *et al*, 1990; Zhou *et al*, 2002). This begets the question on why calcium carbonate is so effective relative to its counterparts. Three reasons have been put forward to explain this; i) Due to its insolubility, calcium carbonate offers the advantage of ‘all at once’ addition thus eliminating the need for a control system for base addition, ii) the presence of calcium carbonate means increased concentrations of bicarbonate (and thereby CO₂), a substrate for pyruvate carboxylase in the carboxylation of pyruvate to oxaloacetate (Zelle *et al*, 2010) and iii), CaCO₃ reacts with the acids present in the broth immediately upon secretion to form insoluble calcium salts of the acids, thus allowing for the production of higher acid concentrations (Kövilein, Umpfenbach & Ochsenreither, 2021; Chi *et al*, 2016). Moreover, some recent studies on *Aspergillus oryzae* have indicated a strong positive correlation between increased CaCO₃ concentrations (much higher than what is required for neutralisation), and malic acid titres and yields (Geyer *et al*, 2018; Kövilein, Umpfenbach, *et al*, 2021). These results cannot be fully explained by the ability of CaCO₃ to offer continuous neutralisation, the increase in bicarbonate concentration, or by the formation of insoluble calcium salts of the acids.

Despite the fact that fumaric acid production by *Rhizopus* species has been extensively studied in CaCO₃-buffered shake flask cultures, to the best of our knowledge, the effect

of increasing CaCO_3 concentrations on the relative production of fumaric and malic acids has not been studied before in *R. delemar*. Preliminary unpublished tests using *R. delemar* showed that increased CaCO_3 concentrations in excess of that required for neutralisation affects the metabolite distribution of *R. delemar*. Based on the work on *A. oryzae* (Geyer *et al*, 2018; Kövilein, Umpfenbach, *et al*, 2021), three factors would be likely be responsible for the observed response. These were insoluble solids, metal ions, and pH (Swart, Ronoh, *et al*, 2022; Zelle *et al*, 2010; Karaffa, Fekete & Kubicek, 2021).

Increased CaCO_3 concentrations consequentially means increased presence of insoluble solids in the fermentation broth. *R. delemar* (zygomycetes fungi) thrive in soils and dead organic matter, and it is therefore likely that increased concentrations of insoluble solids may replicate its natural environment causing changes in its response, compared with when they are submerged in artificial liquid media (Vassilev, 1991). Calcium has been linked to changes in pyruvate carboxylase activity, effects on *fumR* activity, as well as cellular signaling pathways (Zelle *et al*, 2010; Song *et al*, 2011; Y Zhou, 1999). pH control is closely linked to successful acid production in microbial processes. As the pH drops in *R. delemar* mediated fermentation as a consequence of acid production, the rate of fumaric acid production slows down and eventually ceases, necessitating the addition of neutralising agents to prevent this self inhibition. Production of fumaric acid by *R. delemar* is usually performed at neutral pH values. CaCO_3 maintains the pH at around 6.5 in acid forming microbial processes (Salek *et al*, 2015). Increasing CaCO_3 concentrations beyond the amounts required for neutralisation means that pH would be maintained throughout the duration of the fermentation (Gangl *et al*, 1990). In a recent study, Swart *et al* (Swart, Ronoh, *et al*, 2022) found that higher pH conditions (pH 6) were unfavourable for fumaric acid production with *R. delemar*. The findings clearly indicated that the three-fold increase in osmotic and ionic stresses, compared to pH 4 condition, resulted in the production of unwanted by products, including malic acid. Investigation at even higher pH conditions (pH 7) was necessary to further establish these findings.

The aim of this study was to investigate the fumaric and malic acid production capability of *R. delemar* in the presence of CaCO_3 . Shake flask cultivations were utilised to explore the effect of insoluble solids, metal ions, and pH on the relative production of FA and MA in a bid to gain insight into the role of CaCO_3 in fermentations mediated by *R. delemar*. The subsequent experiments were conducted in an immobilised reactor operated continuously with precise pH control to further test the effect of pH and provide a proof of concept on the key findings on a bench scale.

Fumaric acid bioproduction with *R. delemar* has been studied extensively, with most of the focus aimed at achieving the highest titres, yields, and productivities attainable

through the optimisation of the production conditions and the application of genetic engineering tools. However, little is known about the malic acid production capabilities of *R. delemar* as not much research effort has been devoted to understanding the conditions of its production. The findings of this study will help establish the potential for malic acid production, through an uncovering of the mechanisms involved and the specific conditions that enhance MA production in *R. delemar*.

1.1 Outline of the dissertation

Chapter 1

This chapter provides a background on the microbial production of organic acids, and its role in achieving the overarching goal of reducing the dependence on fossil fuels. It also provides a brief overview of fumaric acid production with *R. delemar*, with an emphasis on the various critical parameters explored in literature. The aims and objectives as well as the significance of the study is also included in this chapter.

Chapter 2

This chapter presents the literature review for this work. It is divided into five sections: 1. The transition to a bio-based economy, 2. Microbial conversion of biomass into chemicals, 3. Biocatalysts, 4. Neutralising agents, and 5. Future prospects.

Chapter 3

This chapter outlines the materials, methods, experimental procedures, experimental design, reactor operation, and mass balance. The experimental procedure section is divided into two parts, with the first part detailing the different procedures under shake-flask cultivations, while the second focuses on immobilised reactor cultivations.

Chapter 4

This chapter describes the main findings of this study under six different sections; 1. Biomass, 2. Effect of CaCO₃ addition, 3. Effect of MgCO₃ addition, 4. Effect of plaster sand addition, 5. Effect of calcium ions, and 6. Effect of pH. The results from the last experiments included a variation of the glucose feed rates and a variation of the pH, conducted in a continuous flow system with precise pH control, which further established the findings from the shake-flask cultivations.

Chapter 5

This chapter presents the conclusions based on the results from chapter 4. The recommendations for improving the results reported in this study and for future work are also included in this chapter.

2 Literature review

2.1 The transition to a bio-based economy

2.1.1 Energy

Fossil fuels, including coal, natural gas, and oil are primary sources of energy and account for over 80 % of the world’s energy consumption (Fatih Birol, 2020). Although there has been a significant decline from our fossil fuel dependency from the peak in 1966 (94 %), about 15 billion metric tonnes of fossil fuels are still burned every year throughout the world, a clear indication that energy is one of the most influential and important aspect of modern society (Dinçer, 2018). While the debate on when we shall run out of these finite resources is ongoing, it is abundantly clear that as economies continue to develop and the world’s population increases, there will be an inevitable increase in energy demands, consequentially resulting in an even faster depletion of the remaining fossil resources. Figure 1 illustrates the global primary energy consumption by source over the past two centuries.

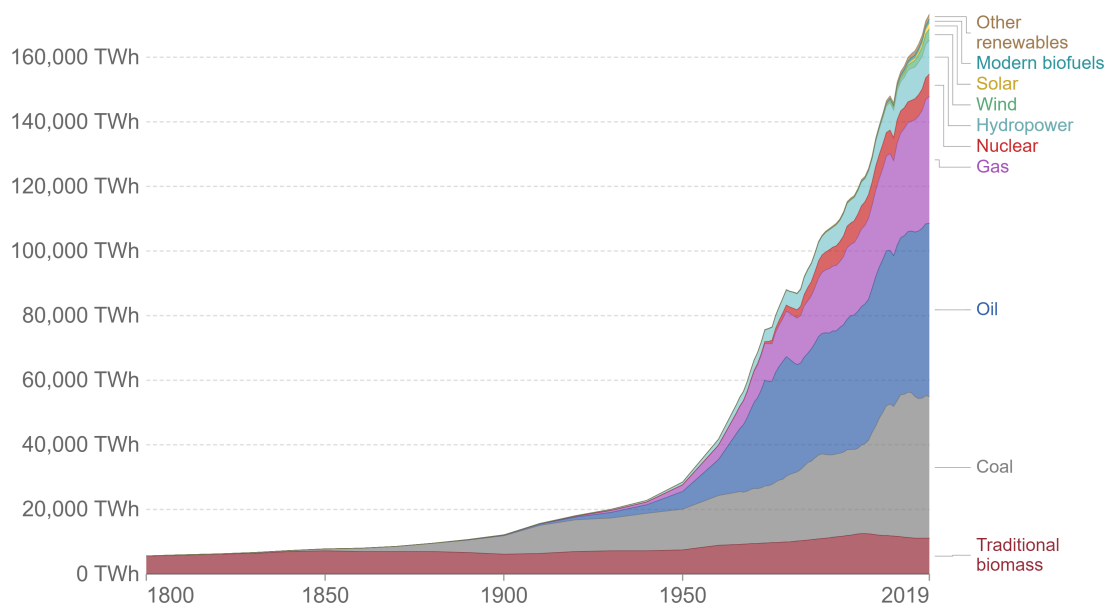


Figure 1: Global primary energy consumption by source (Fatih Birol, 2020). IEA 2020; *Key World Energy Statistics*, <https://www.iea.org/reports/key-world-energy-statistics-2020>, License: CC by 4.0 International.

Besides higher availability, fossil fuels dominate the energy market largely because they are energy dense and historically relatively cheap. Natural gas for example has an energy density of 40 million joules per cubic meter, compared to the 0.05 joules per cubic meter

contained in geothermal energy (Layton, 2008). However, with the convenience of their exploitation also came a myriad of challenges we face today, including pollution of the environment and global warming.

Renewable energies are set to inevitably dominate the world's energy supply in the long run. The reason is both very simple and imperative: there is no alternative. Mankind cannot base its life on the consumption of finite energy indefinitely. Though humans have been tapping into most renewable energy sources (wood, solar, wind, geothermal, and water) for thousands of years for their needs, so far only a tiny fraction of the technical and economic potential of renewable energy has been captured and exploited. Yet, with existing and proven technologies, renewable energies offer safe, reliable, clean, local, and increasingly cost-effective alternatives for all our energy needs. The renewable energy sector has become a driving force for a sustainable economy in the 21st century (Jones & Mayfield, 2016).

Combined with improvement in the energy efficiency and the rational use of energy, renewable energy sources can provide everything fossil fuels currently offer in terms of energy services such as heating, lighting, cooking, refrigeration, cooling, and water heating. Although none of the developed technologies can solely fulfill our current energy needs, there lies massive potential in the implementation of an integrated approach combined with a general concern for energy saving and improved energy-efficient technologies, which if correctly done can go a long way in shifting our conventional way of living towards sustainability (Lund, 2007; Vanholme *et al.*, 2013).

2.1.2 Chemicals and materials

Fossil fuels are also used as feedstock in the manufacturing of chemicals and materials for variety of widely used products such as plastics, fertilisers, detergents, and tyres. While commonly neglected in the global climate mitigation debate, the chemical industry accounts for 14 % of the total primary demand for crude oil and 8 % for natural gas (Agency, 2019). In 2008 for example, an estimated 4 % of the total fossil fuel extracted was used as a raw materials for plastics (Lebreton & Andrady, 2019). With the ever-increasing demand owing to its unrivaled functional properties and low cost, it is projected that by the year 2050, plastics manufacturing and processing may account for as much as 20 % of petroleum consumed globally and 15 % of the annual carbon emissions budget (Lebreton & Andrady, 2019; World Economic Forum, 2016). This, coupled with the unsustainable plastic waste production that is crippling vital natural system, provides an incentive for the envisioning of a new plastic economy with various innovative solutions,

including a switch to biomass feedstock to make bioplastics that include the most-used synthetic plastic, polyethylene (Lebreton & Andrady, 2019).

Moreover, the utilisation of biomass resources to produce commodity chemicals has recently received increased attention for sustainable development, mainly due to its renewability as well as environmental benefits particularly with regards to the reductions of greenhouse gas (GHG) emissions compared to fossil resources (Kikuchi, Kanematsu & Okubo, 2016). With the advancement of biotechnology, many chemicals that were produced solely by chemical processes from petroleum-based materials in the past now have the potential to be produced from biomass (Ji, Huang & Ouyang, 2011; Xu *et al.*, 2012)

2.1.3 Transportation fuels

The increase in globalisation has been associated with shifts in the energy consumption patterns, clearly observable in the growing share of transportation in total energy consumption. In only a span of 45 years, the share of total energy consumed by the transport sector has risen from 24.2 % to 33.7 % (Figure 2). This is mainly attributed to the growing level of motorisation including the growth of international trade (maritime shipping and air transportation) (Rodrigue, Comtois & Slack, 2009).

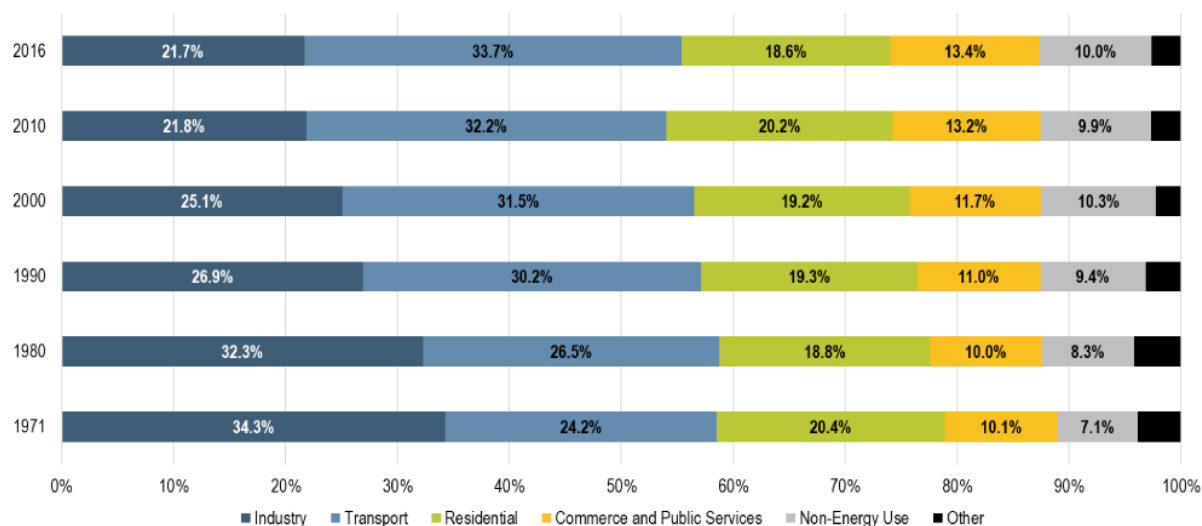


Figure 2: Energy Consumption by Sector, OECD Countries (International Energy Agency). IEA 2020; *Energy Technology Perspectives 2020 - Special Report on Clean Energy Innovation*, <https://www.iea.org/reports/energy-technology-perspectives-2020>, License: CC by 4.0 International.

No discussion on a zero-emissions future is complete without addressing the emissions from the transport sector. Notorious for the difficulty in decarbonisation, the transport

sector accounts for 21 % of total emissions, and road transport accounts for three-quarters of transport emissions (IEA, 2020). There is therefore a big incentive to develop usable biofuels that can replace the existing petroleum-based fuels. Two unique advantages already exist that could be easily harnessed to ensure a smooth transition: 1) biomass is easy to store until when required, and 2) the biofuel(s) produced can be easily integrated into the existing transportation fuel systems (Merckel, 2014). Most of the biomass-based diesel consumption is in blends with petroleum diesel.

While it is clear that biofuels are the only feasible renewable resources that can address our over-reliance on fossil fuel oils in the transport sector and aid in mitigating the resultant emissions, there is still a long way off from realising its potential. This is reflected in the transport sector data, with biofuels consumption accounting for only about 5% of the total US transportation sector energy consumption in 2020 (Figure 3).

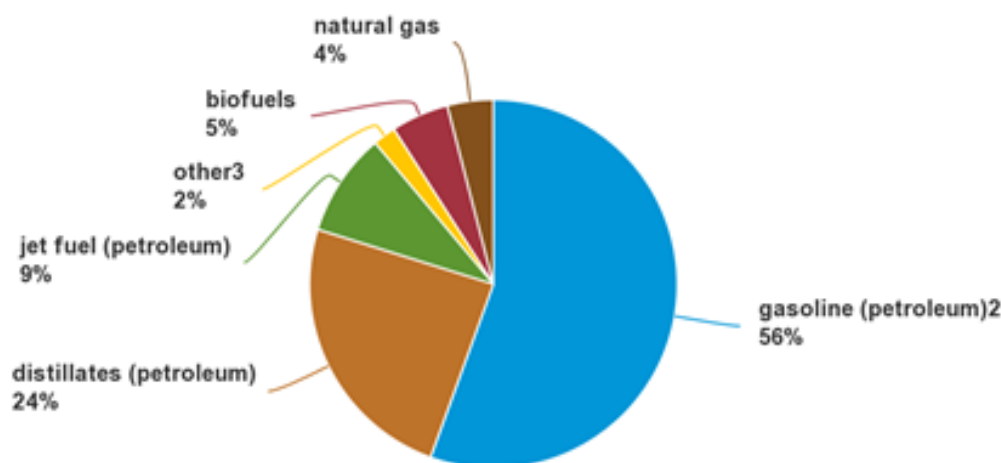


Figure 3: Transportation energy sources/fuels in 2020. Source: U.S. Energy Information Administration (April 2020)

2.2 Microbial conversion of biomass into chemicals

As established, the majority of chemicals are currently produced from fossil petroleum. The growing need to find alternative processes to produce these very chemicals has led many researchers back to exploring microbial conversion, an industry that was partially developed in the 1940s, but swiftly abandoned with the advent of the less expensive petrochemical methods (Roa Engel, Straathof, *et al*, 2008). The renewed interest in microbial conversion of biomass into chemicals resulted in leading institutions such as the U.S. Department of Energy (DOE) and the European Commission ordering a study around the sustainable production of chemicals from renewable resources (Beauprez, De

Mey & Soetaert, 2010). One key output of the DOE study in 2004 was the identification of 12 chemical building blocks obtainable from biomass as potential platform chemicals; meaning that they can be converted to a number of high-value bio-based chemicals or materials (Werpy & Petersen, 2004). Four carbon 1,4-diacids (fumaric, malic, succinic) are among these top 12 building blocks identified.

2.2.1 Fumaric acid

Fumaric acid is an important specialty chemical with wide industrial applications ranging from its use as feedstock for the synthesis of polymeric resins to acidulants in food and pharmaceuticals (Ding *et al*, 2011). Compared to other dicarboxylic acids, fumaric acid has low aqueous solubility (7 g kg^{-1} at 25°C ; 89 g kg^{-1} at 100°C) and low pKa values (3.03 and 4.44), which are properties that can be exploited for product recovery (Roa Engel, Straathof, *et al*, 2008). Fumaric acid is 1.5 times more acidic than citric acid and is therefore commonly used as a food acidulant and beverage ingredient (Ding *et al*, 2011). While the second application by volume is in the paper and pulp industry as an acid sizing agent, a progressive change to alkaline processing of wood to paper on North America and Europe is slightly reducing the reliance on fumaric acid in this regard (Martin-Dominguez, Estevez, *et al*, 2018).

Additionally, fumaric acid is widely used in the feed industry as an antibacterial agent and a physiologically active substance (Xu *et al*, 2012). Fumaric acid has a double bond and two carboxylic groups that can be polymerized to produce synthetic resins, biodegradable polymers, and plasticisers (Roa Engel, Straathof, *et al*, 2008; Sebastian *et al*, 2019). In addition, special properties such as greater hardness in the polymer structure can be achieved when fumaric acid is used. As an important platform chemical, fumaric acid is a valuable intermediate in the preparation of edible products, such as L-malic acid and L-aspartic acid (Goldberg *et al*, 2006). With the increasing market share of L-aspartic acid and L-malic acid in sweeteners, beverages, and other health food areas, the worldwide demand for fumaric acid and its derivatives grows each year (Xu *et al*, 2012).

More recently, derivatives of fumaric acid, especially fumaric acid esters have found application as important chemicals with a wide array of biomedical applications, such as psoriasis and sclerosis treatment and a support material for tissue engineering (Sebastian *et al*, 2019). Another potential application of fumaric acid is as supplement in piglet, broilers, and cattle feed (Lan & Kim, 2018; Patten & Waldroup, 1988; Beauchemin & McGinn, 2006). Recent studies indicate that a large reduction in the methane emissions of cattle can be achieved (up to 70%), if these cattle receive fumaric acid-based additive as a supplement in their diet (McGinn *et al*, 2011). This could greatly reduce the total

emission of methane, as farm animals are responsible for 14 % of the methane emission caused by human activity.

Fumaric acid, also known as (E)-2-Butenedioic acid, was first isolated from the plant *Fumaria officinalis*, from which it derives its name (Roa Engel, Straathof, *et al*, 2008). The structure and functional groups of fumaric acid make it a versatile chemical. It has two terminal carboxylic acid groups and a double bond in the α , β position as shown in Figure 4. The structure positions fumaric acid between maleic acid and succinic acid since fumaric acid can easily be isomerised to maleic acid or hydrogenated to succinic (Swart, Le Roux, *et al*, 2020).

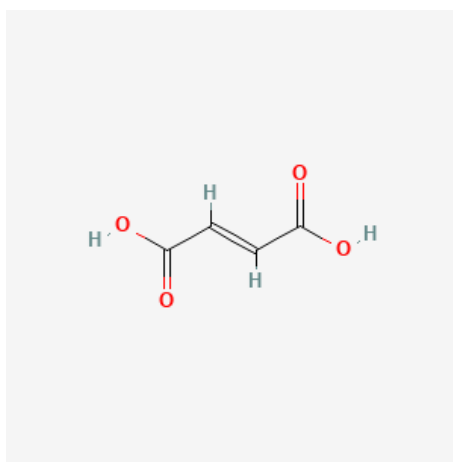


Figure 4: Fumaric acid structure. National Center for Biotechnology Information (2022). PubChem Compound Summary for CID 444972, Fumaric acid. Retrieved April 28, 2022 from <https://pubchem.ncbi.nlm.nih.gov/compound/Fumaric-acid>.

Many microorganisms produce fumaric acid in small amounts as it is a key intermediate in the citrate cycle. In a 1938 study by Foster & Waksman (1939), 41 strains from 8 different genera were screened to identify high fumarate producing strains. The identified fumarate producing genera were *Rhizopus*, *Cunninghamella*, *Mucor*, and *Circinella* species. Among these strains, *Rhizopus* species were highlighted as the most prolific fumaric acid producers (Kenealy, Zaady & Du Preez, 1986; Cao *et al*, 1996; Gangl *et al*, 1990; Rhodes, Moyer, *et al*, 1959; Roa Engel, Straathof, *et al*, 2008).

2.2.2 Malic acid

Malic acid (2-hydroxybutanedioic acid) is a C4-dicarboxylic acid and an intermediate in the tricarboxylic acid (TCA) cycle. It can be used in the chemical industry as a feedstock for chemical synthesis of polymalic acid (PMA), which can be applied as biodegradable plastic (Chi *et al*, 2016; Dai *et al*, 2018). However, the main use for malic acid is as an acidifier in the food and beverage industry where it is preferred to fumaric acid because of

the increased solubility, and to citric acid because of the increased acidity. It is the second most used acidulate after citric acid and holds 10 % of the market share. Other utilisations include electrode-less plating, pharmaceuticals, textiles finishing, metal finishing, and paint infusions (Goldberg *et al*, 2006).

In agriculture, malic acid is utilised to solubilise aluminum phosphate in soil. At a soil pH below 5.5, aluminum more readily reacts with phosphates. The lack of water solubility of aluminum phosphates means that these compounds are not readily available for plant use, thus the need for malic acid application (West, 2017). In the cosmetic industry, malic acid is included in many products such as self-tanning cream, facial cream, and cleansing foam, mainly to adjust pH in a low concentration. Malic acid is also often included in soaps, mouthwisher fluids, and toothpaste as it can diminish the flavors of active chemicals. Macromolecular materials from L-malic acid have found uses in the biomedical industry, with adjustments for structure and properties (Lee *et al*, 2011). L-malic acid can also be used as a precursor of amino acid infusions for the treatment of hyper-ammonemia and liver disfunction (Peleg *et al*, 1989).

Malic acid contains three types including D-, L-malic, and mixture of DL-malic acid based on the optical isomer of a symmetric carbon atom which plays different roles in practical applications (Dai *et al*, 2018). Currently, the majority of malic acid synthesised by chemical means through the hydration of fumaric acid under high temperature and pressure results in the racemic mixture of D and L malate (Kövilein, Kubisch, *et al*, 2019; Chi *et al*, 2016). This racemic mixture is mainly applied mainly in the food, beverage, personal care, and cleaning product industries. For applications that are as specific as in the pharmaceutical industry or polymer production, enantiopure malic acid is preferred. However, resolution of the racemic mixture produced by the chemical method is quite expensive and therefore unsuitable for large-scale implementation (Kövilein, Kubisch, *et al*, 2019). The need for sustainable production of enantiopure L-malic acid has driven many research efforts into the exploration of alternative production methods.

Malic acid can be naturally accumulated by various microorganisms and plants. First isolated from apples in 1785, malic acid is the predominant acid in many fruits, including plums, bananas, and litchis (Kövilein, Kubisch, *et al*, 2019). Although previously extracted industrially from fruits and eggshells, these processes were deemed uneconomical as fruit juices comprise of less than 1 % L-malate, and extraction from eggshells brought with it a battery of problems including low extraction rates, high energy consumption, high cost and heavy pollution (Chi *et al*, 2016; Lin & Luque, 2014).

Bio-based production of malic acid is superior to chemical synthesis in two main aspects: 1) Only enantiopure L-form of malic acid is produced, and 2) the versatility and inde-

pendence from fossil fuels, given that microbial fermentations can employ a wide variety of microorganisms that utilise a large range of substrates (Jang *et al*, 2012; Kövilein, Kubisch, *et al*, 2019). Although malic acid is part of the TCA cycle, it does not always accumulate in every organism and under normal conditions and therefore certain species are well known for their ability to produce and accumulate malic acid in large quantities, both natively and through metabolic engineering. *Aspergillus* species (*flavus*, *niger*, *oryzae*, *citricus*) are the most prolific malic acid producers currently known.

The current market volume of malic acid ranges between 60 000 and 200 000 ton per year, and is predicted to increase in the coming years. With the prospect of the transition to a bio-based economy, malic acid has the potential to replace maleic anhydride, a commodity chemical currently solely produced by chemical means, and with a global market of 1.5 to 2 million ton per year (Kövilein, Kubisch, *et al*, 2019).

2.3 Biocatalysts

Fungal species have been employed to produce a vast array of compounds and consumables. Multicellular filamentous fungi or moulds are extensively used to produce fermented foods, secondary metabolites, and industrial enzymes. *Rhizopus* is an example of filamentous fungi, belonging to the 'Mucoraceae' family, that is used to generate a wide array products ranging from fermented food products to alcohols, and enzymes, and organic acids in large quantities (Sebastian *et al*, 2019).

The question then is why *Rhizopus* species (and other filamentous fungi) produce these seemingly ridiculous quantities of organic acids. Several hypotheses have been suggested, with the main two as follows: Fungi in their natural habitats would not typically encounter free sugars in such high concentrations as they are exposed to in experiments for industrial applications, and as a consequence may not have developed a tight regulation of acid production. Therefore, when exposed to artificial media with high concentrations of free sugar, they engage in excessive acid production eventually resulting in their own demise. Another school of thought is that acid production actually confers a competitive advantage through the chelation properties (allowing growth in areas with low metal concentrations), and growth inhibition of competitors (Vassilev, 1991).

2.3.1 *Rhizopus delemar*

Rhizopus delemar is a prominent Zygomycetes fungus that is ubiquitous in nature and found in soils and decaying organic materials. It has the ability to grow on a wide array of

substrates including glucose, glycerol, ethanol, xylose, lactic acid, fructose, mannose, sucrose, and cellobiose (Meussen *et al*, 2012). Moreover, *R. delemar* has a well demonstrated growth ability in a vast array of culture media, with requirements generally characterised as inexpensive and unspecific. *R. delemar* can be used for human consumption in the U.S. and other parts of the world as it is considered GRAS (Generally Recognized As Safe) by the U.S Food and Drug Administration (FDA).

Rhizopus delemar strains can be divided into two types based on the primary organic acid produced when grown on D-glucose (Meussen *et al*, 2012). The first strain primarily produces L-(+)-lactic acid is classified as Type I. This strain contains both *ldhA* and *ldhB* genes and were confirmed as phylogenetically distinct from the fumaric-malic acid producing strain (Type II), which only contains *ldhB* gene. Abe, Sone, *et al* (2003) then proposed the reclassification of the latter strain (Type II) to *R. delemar*. However, the name has not been widely adopted in literature, as many studies still refer to both strains as *R. oryzae*.

2.3.2 Carbon metabolism

Fumaric and malic acids are well known as intermediates of the TCA cycle, but they are also involved in other pathways in *Rhizopus* species. In 1967, Overman & Romano (1969) first put forward the hypothesis that the reductive TCA cycle was responsible for the majority of fumaric acid accumulation through a C3 plus C1 mechanism for the fixation of CO₂ (Xu *et al*, 2012). Later studies on the ¹³C nuclear magnetic resonance and enzymatic activity confirmed this mechanism (Kenealy *et al*, 1986; Peleg *et al*, 1989).

All fermentable carbon in *R. delemar* are first metabolised to pyruvate. The pyruvate can thereafter be channeled through three main pathways; namely, ethanol production, TCA cycle, and the reductive TCA cycle used to generate fumarate (Meussen *et al*, 2012). The latter is exclusively located in the cytosol (Osmani1985). Figure 5 shows the metabolic pathways in *R. delemar*. The maximal theoretical molar yield of fumaric acid from glucose is 200 % due to CO₂ fixation in the reductive part of the TCA cycle (Zhang, Yang, *et al*, 2012). However, significantly lower yields are often attained experimentally as a consequence of the energy production in the form of ATP or GTP and reducing power in the form of NADH₂ or FADH₂ in the oxidative TCA cycle. The above-mentioned processes are critical to meeting the energy requirements for cell maintenance and acid transport (Xu *et al*, 2012; Kenealy *et al*, 1986; Gangl *et al*, 1990; Rhodes, Moyer, *et al*, 1959).

The biosynthesis of fumarate and malate in the cytosol occurs by the aid of three re-

actions catalysed by pyruvate carboxylase, malate dehydrogenase (MDH), and fumarase (FUM). Pyruvate carboxylase is the first enzyme of the reductive TCA pathway, and it is exclusively located in the cytoplasm, where it catalyses the carboxylation of pyruvate to oxaloacetate with the participation of ATP and CO₂ (Xu *et al*, 2012). Malate dehydrogenase thereafter converts the oxaloacetate to malic acid, which is then hydrated reversibly to fumaric acid by the enzyme fumarase (Meussen *et al*, 2012). Friedberg *et al* (1995) postulated that the reason behind the accumulation of fumaric acid by *R. delemar* is that a unique FUM induced under acid production conditions would produce fumaric acid, and the reverse reaction would be inhibited by increased concentrations of fumaric acid (above 2 mmol L⁻¹). Fumarase is believed to be encoded by a single gene *fumR* and it catalyses the reversible dehydration of L-malic acid to fumaric acid. Zhang, Yang, *et al* (2012) attempted to increase fumaric acid production by overexpressing *fumR*. However, their findings showed that overexpressing *fumR* increased the fumarase activities of both reaction directions and led to the conversion of fumaric acid to L-malic acid, resulting in a malic acid yield of 0.38 ± 0.07 g g⁻¹ glucose. These results not only establish that the overexpressed fumarase is not responsible for fumaric acid production, but is also a crucial basis from which we can explore the malic acid production capabilities of *R. delemar*.

Previous studies have been conducted on enzymatic production of L-malic acid, applying the enzyme fumarase which converts the substrate fumaric acid to malic acid through hydration. This has been done by using either purified fumarase enzyme, permeabilized or lyophilized cells, or whole cells, with the latter being the most widely used method. With whole cell catalysis, the cells are preferably immobilised in suitable materials in order to make the process more economical by allowing for catalyst reutilisation (Kövilein, Kubisch, *et al*, 2019). Using this process, Naude & Nicol (2018) was able to produce malic acid through the enzymatic whole-cell bioconversion using *R. delemar* (ATCC 20344) taking advantage of the absolute specificity of fumarase towards L-malic.

In a thermodynamics research study, Tewari *et al* (1986) found the Gibbs free energy, $\Delta G_0'$, of the conversion of L-malic acid to fumaric acid is 3.6 kJ mol⁻¹, indicating that at equilibrium, the L-malic acid concentration is higher than the fumaric acid concentration. The implication here is that a dicarboxylic acid transporter with a high selectivity for fumaric acid plays a critical role in the production of fumaric acid in *R. delemar* (Meussen *et al*, 2012).

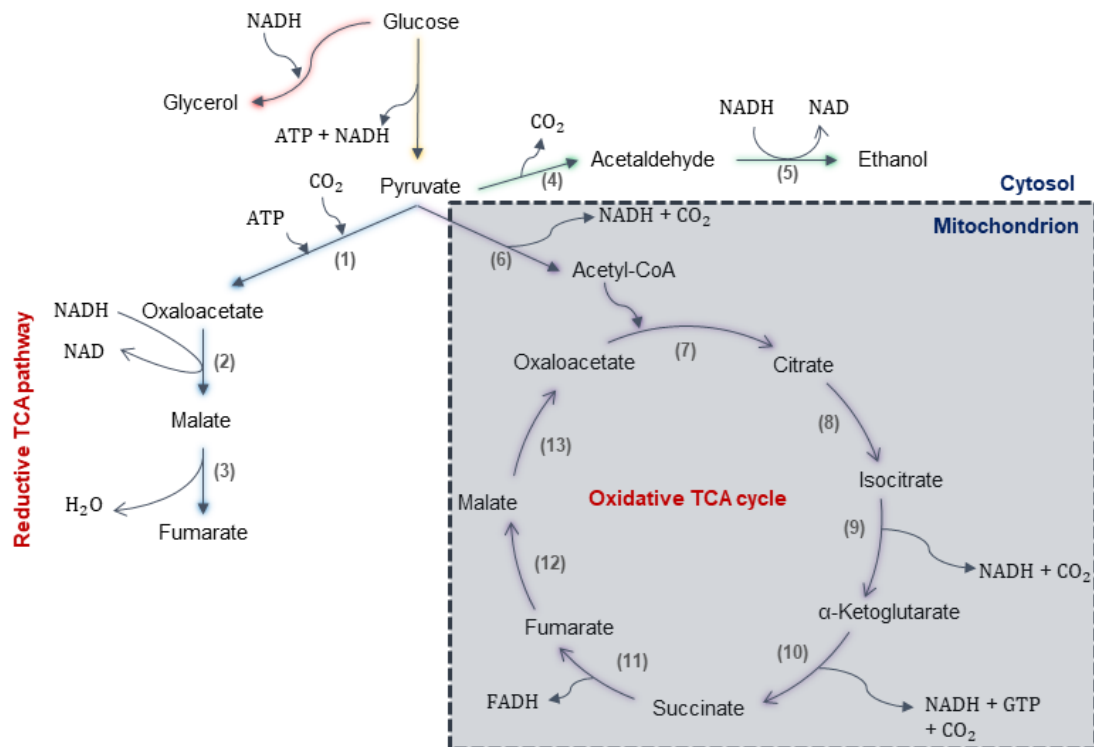


Figure 5: Metabolic pathways of *Rhizopus delemar* (adapted from Naude & Nicol (2017)). Enzymes are indicated by bracketed numbers: 1. Pyruvate carboxylase, 2. Malate dehydrogenase, 3. Fumarase, 4. Pyruvate decarboxylase, 5. Alcohol dehydrogenase, 6. Pyruvate dehydrogenase complex, 7. Citrate synthase, 8. Aconitase, 9. Isocitrate dehydrogenase, 10. α -ketoglutarate dehydrogenase and succinyl-CoA synthase, 11. Succinic dehydrogenase, 12. Fumarase, 13. Malate dehydrogenase

2.4 Neutralising agents

pH is the most important condition in the production of acids by fermentation, and in the biotechnological process in general, due to its regulatory effect on microorganism activities (Martin-Dominguez, Estevez, *et al*, 2018). Fumaric acid production by fermentation has usually been carried out with *Rhizopus delemar* around neutral pH values, leading to fumarate salts (Roa Engel, Van Gulik, *et al*, 2011). In *Rhizopus*-mediated fumaric acid production, the pH value quickly drops from 5.0 to 2.0 in the first 20 h without the addition of a neutraliser control, and this acidification exerts a progressively inhibitory effect on growth and fumaric acid production (Roa Engel, 2010). To avoid the inhibition, it is critical to use a neutralising agent. Malic acid has pK_{a1} and pK_{a2} values of 3.51 and 5.03 respectively, and with the low pK_a values of fumaric acid, small amounts of both acids can decrease the pH of the medium considerably (Swart, Le Roux, *et al*, 2020).

2.4.1 CaCO₃

Calcium carbonate (CaCO₃), as a solid powder, is the most widely used neutralising agent in industry. In lactic acid production, CaCO₃ is added during fermentation, and in citric acid production, CaCO₃ is added after fermentation. In fumaric and malic acid production with *R. delemar*, three benefits of using CaCO₃ are highlighted as follows: 1) all at once addition, discarding the need for pH control, 2) increased presence of bicarbonate, and thereby CO₂, a substrate for pyruvate carboxylase in the carboxylation of pyruvate to oxaloacetate leading to increased yields (in theory), and 3) formation of insoluble calcium salts of the organic acids secreted, allowing for the production of higher acid concentrations. CaCO₃ is considered to be the most efficient in commercial fumaric acid production (Xu *et al*, 2012; Gangl *et al*, 1990). Studies comparing calcium carbonate to other neutralising agents such as calcium hydroxide, sodium carbonate, and sodium bicarbonate have consistently achieved higher product titres and yields in fermentations with CaCO₃ (Zhou *et al*, 2002; Gangl *et al*, 1990). It was noted that most calcium carbonate mediated fermentations reported in literature utilised a lot more calcium carbonate than was required for neutralisation, an indication that increasing concentrations of CaCO₃ likely has an effect on the acid production mechanism in *R. delemar*.

However, the use of CaCO₃ as a neutralising agent also causes viscosity problems due to the low aqueous solubility of calcium fumarate (21 g L⁻¹ at 30 °C) (Gangl *et al*, 1990). Moreover, cells interact with the precipitated product to form a highly viscous suspension that can cause early failure of the fermentation due to limited oxygen transfer. This has prompted many research efforts to turn to more soluble alternatives such as Na₂CO₃, NaHCO₃, and NaOH.

In an economic feasibility study contrasting the utilisation of CaCO₃ and Na₂CO₃ as neutralising agents, Gangl *et al* (1990) highlighted that while Na₂CO₃ costed 20 % more than purified CaCO₃, the fumaric acid productivities as reported in the literature for Na₂CO₃ fermentations were significantly lower. However, it was determined that the increased costs from using Na₂CO₃ could be offset by the reduced downstream processing costs as well as the possibility for cell re-use thereby increasing the yield and productivity (Gangl *et al*, 1990; Zhou *et al*, 2002). NaOH has also been flagged as a worthy alternative to CaCO₃ given that it is also very soluble and that there is little to no inhibition of the salt on the organism. However, when a high yield process is developed without a carbonate as a neutralising agent, the required CO₂ must be supplied by other sources (Roa Engel, Straathof, *et al*, 2008). Table 1 shows the comparison of the effects of neutralising agents CaCO₃ on fumaric acid production by *Rhizopus delemar*.

Table 1: A comparison of the effect of different neutralising agents on fumaric acid production with *R. delemar*

Neutralising agent	Process	pH range	Yield (g g ⁻¹)	Productivity (g L ⁻¹ h ⁻¹)	Reference
CaCO ₃	Stirred tank	5.5-6.8	0.82	2.00	Ng <i>et al</i> (1986)
CaCO ₃	Stirred tank	-	0.70	1.22	Rhodes, Lagoda, <i>et al</i> (1962)
CaCO ₃	Stirred tank	5.5	0.54	0.70	YQ Fu <i>et al</i> (2010)
CaCO ₃	Bubble column	5.5	0.53	1.03	Zhou, Du & Tsao (2002)
CaCO ₃	RBC	5.0	0.75	3.78	Cao (1997)
CaCO ₃	Shake flask	-	0.58	0.56	H Liu <i>et al</i> (2017)
CaCO ₃	Shake flask	4.0	0.33	0.35	Q Xu <i>et al</i> (2010)
CaCO ₃	Shake flask	5.0	0.40	0.227	Zhang, Yang, <i>et al</i> (2012)
CaCO ₃	Air lift	5.0	0.75	0.81	Jianxin (1997)
CaCO ₃ + CO ₂	Shake flask	5.0	0.40	0.40	Zhang, Yang, <i>et al</i> (2012)
Ca(OH) ₂	Bubble column	5.5-5.6	0.173	0.0.26	Zhou, Du & Tsao (2002)
Na ₂ CO ₃	Stirred tank	5.5	0.72	0.50	Gangl, Weigand & Keller (1990)
NaHCO ₃	Bubble column	5.5-5.6	0.337	0.69	Zhou, Du & Tsao (2002)
NaOH	Immobilised reactor	4.0	0.93	0.305	Swart, Ronoh, <i>et al</i> (2022)
NaOH	Immobilised reactor	5.0	0.81	0.30	Naude & Nicol (2018)
NaOH	Shake flask	5.0	0.39	0.223	Zhang, Yang, <i>et al</i> (2012)
NaOH + CO ₂	Shake flask	5.0	0.38	0.286	Zhang, Yang, <i>et al</i> (2012)

2.5 Future prospects

The ever increasing demand for platform chemicals, the increasing concern for the global environment and the ensuing sustainability requirements as well as high raw material costs have incentivised the research into more efficient alternatives in the form of biocatalysts (Meussen *et al*, 2012). *R. delemar* is a key biocatalyst, well known for its ability to sustainably produce L-lactic acid and fumaric acid in high quantities. Moreover, recent studies have shown a glimpse of its malic acid production capabilities through the enzymatic hydration of fumaric acid derived from petrochemicals using fumarase (Naude & Nicol, 2018).

Gangl *et al* (1990) established that the fermentation route would become profitable when the selling price of fumaric acid is high because of high benzene costs. Given that the cost of benzene is linearly related to the cost of crude oil, they predicted from extrapolation of cost data from 1988, that the cost of crude oil would have to reach \$61/bbl for benzene and fermentation routes to give the same return on investment. This value is approximately 40 % lower than the price of crude oil in February 2022 (\$97/bbl), an indication that fermentation route is fast becoming the more desirable alternative. The most significant future application of fermentation-based fumaric and malic acid production will be the production of maleic anhydride, which has quite a substantial market size but is almost exclusively derived from petroleum-based materials.

3 Experimental

3.1 Materials and methods

3.1.1 Microorganism

The organism used for this study was *R. delemar* (ATCC 20344 or CECT 2774), obtained from the Spanish collection of cultures (Colección Espanola de Cultivos Tipo, Valencia, Spain). All chemicals used were obtained from Merck (Modderfontein, South Africa).

3.1.2 Inoculum preparation

The spore solution was prepared using the following procedure. Potato dextrose agar (PDA) plates were first prepared and dried aseptically as higher spore concentrations resulted when moisture was removed from the plates before inoculation. The stock cultures were stored at $-40\text{ }^{\circ}\text{C}$ in a 50 % w/w glycerol solution. The dried PDA plates were then inoculated with the sub-zero stock solution, sealed shut, and incubated at $30\text{ }^{\circ}\text{C}$. After 120 h, the spores were suspended in distilled sterile water, and rehydrated at $25\text{ }^{\circ}\text{C}$ for a period of at least 18 h before inoculation into the pre-culture. This rehydration step was critical in the growth rate and size of pellets that resulted. The spore inoculum used for the pre-culture for biomass growth had a spore concentration of $8 \times 10^6\text{ mL}^{-1}$.

3.1.3 Shake Flask Cultivations

3.1.3.1 Pre-Culture for Biomass Formation

A two-stage fermentation method was implemented, consisting of a pre-culture for biomass production and a main culture for acid production (Kövilein, Umpfenbach, *et al*, 2021; Roa Engel, Van Gulik, *et al*, 2011). The main difference between the two media was the concentrations of the nitrogen source, with the former having a high nitrogen supply to favour cell growth. The pre-culture medium consisted of (in units of g L^{-1}) 30 glucose, 2 urea, 0.6 KH_2PO_4 , and 0.5 $\text{MgSO}_4 \cdot 7\text{H}_2\text{O}$ (Zhang, Yu & Yang, 2015). Components were autoclaved separately at $121\text{ }^{\circ}\text{C}$ for 1 h and thereafter were mixed aseptically. Unless otherwise indicated, all pre-cultures were prepared in cotton-covered 250 mL unbaffled Erlenmeyer flasks, each containing 50 mL pre-culture media and inoculated with the rehydrated spore suspension (2 mL each). The pre-cultures were carried out in a gyratory

incubator shaker at 200 RPM and 34 °C for 24 h. The cells from each flask in the pre-culture were used for different fermentations in the main culture, i.e., no mixing of cells occurred between the two fermentation stages.

3.1.3.2 Main Culture for Acid Production

Batch fermentations were studied in the same 50 mL unbaffled Erlenmeyer flasks. Unless otherwise noted, the switch to production followed this procedure: 30 mL of the pre-culture media (inclusive of the cells) was transferred into 90 mL of the fermentation media for each flask, resulting in a final composition (in units of g L^{-1}) of 100 glucose, 0.8 KH_2PO_4 , and 0.6 $\text{MgSO}_4 \cdot 7\text{H}_2\text{O}$ (Zhang, Yu, *et al.*, 2015).

For the initial CaCO_3 experiments, CaCO_3 concentrations were varied within 20–100 g L^{-1} , and all experimental conditions performed in triplicate. All components were sterilised separately by autoclaving at 121 °C for 1 h. The main cultures were carried out in a gyratory incubator shaker at 200 RPM and 34 °C for around 200 h. The pH was measured and recorded at the end of the cultivation period.

In all subsequent experiments, pre-culture conditions were kept exactly the same. Further experiments conducted to compare CaCO_3 to MgCO_3 involved similar mass-based amounts of alkali for ease of comparison of the resultant data. Three different CaCO_3 and MgCO_3 concentrations were tested, 20, 60, and 100 g L^{-1} , with all conditions performed in triplicate. All fermentations had an initial substrate (glucose) concentration of around 100 g L^{-1} .

Plaster sand (PS) was used to simulate the conditions in the fermentation broth with CaCO_3 and MgCO_3 buffered cultures. A sieve analysis was conducted to compare the particle size distribution of plaster sand and CaCO_3 , by determining the amount of particles retained on a nest of sieves with differently sized apertures, ranging from 0.075 to 2 mm. As the sieves vibrated, the sample was segregated onto the differently sized sieves, and the weight of sample retained and then used to determine the particle size distribution. Given the need for pH control, a baseline amount of 20 g L^{-1} was used for all conditions tested. In addition to the baseline CaCO_3 , three different concentrations of PS were tested: 40, 80, and 120 g L^{-1} .

Tests on the effect of calcium ions were conducted using a similar procedure with 20 g L^{-1} used as the baseline amount (for pH control) and additional amounts of 5, 10, and 20 g L^{-1} calcium ions added to the baseline in the form of CaCl_2 . All other fermentation conditions were maintained as described earlier.

3.1.4 Immobilised Reactor Cultivations

3.1.4.1 Medium

A 10 M NaOH solution was used as pH control to minimise dilution (Swart, Le Roux, *et al.*, 2020; Naude & Nicol, 2017). The inoculum, consisting of a 10 mL solution containing 8×10^6 spores mL⁻¹, was aseptically injected into the reactor through a silicon septum. Biomass was grown under batch conditions with 3.1 g L⁻¹ glucose and 2.0 g L⁻¹ urea (Swart, Le Roux, *et al.*, 2020). The minimal medium for continuous production contained (in units of g L⁻¹) 0.6 KH₂PO₄, 0.507 MgSO₄ · 7 H₂O, 0.0176 ZnSO₄ · 7 H₂O, and 0.0005 FeSO₄ · 7 H₂O (Y Zhou, Du & Tsao, 2000). Glucose and urea were absent in the minimal media as they were fed continuously into the reactor during the course of the production run. High glucose and urea concentrations (340 g L⁻¹ and 16 g L⁻¹, respectively) were utilised to achieve low dilution rates during the production phase. All solutions were autoclaved at 121 °C for 60 min (Swart, Le Roux, *et al.*, 2020).

3.1.4.2 Reactor Operation and Experimental Design

An immobilised reactor was used with a liquid volume of 1.08 L and a gas volume of 0.380 L. The reactor design was adapted from previous research work on fumarate production by immobilised *R. delemar* (Naude & Nicol, 2017; Swart, Le Roux, *et al.*, 2020). All growth phases were controlled at a pH of 5. Urea was fed at a constant rate of 0.625 mg L⁻¹ h⁻¹ for all the experiments. Further information on the reactor operation can be found in the previous research studies (Naude & Nicol, 2017; Swart, Le Roux, *et al.*, 2020; Jongh, Swart & Nicol, 2021; Swart, Ronoh, *et al.*, 2022).

All fermentations were performed in two separate stages: the aerobic growth of the fungus, followed by an aerobic non-growth production stage induced by nitrogen limitation. Medium replacements were done between the growth phase and the production phase. Experiments on the effect of glucose feed rates and pH were conducted by throttling glucose feed rates between 0.131 g L⁻¹ h⁻¹ and 0.329 g L⁻¹ h⁻¹. The glucose feed rate was increased from 0.131 g L⁻¹ h⁻¹ to 0.329 g L⁻¹ h⁻¹, with the duration of around 36 h between each increment. The production phase was conducted for around 200 h. The glucose feed rates were tested across cultures maintained at four different pH conditions: 4, 5, 6, and 7. This was well within the pH range in which *R. delemar* is able to withstand (Meussen *et al.*, 2012).

The next set of experiments (pH steps) involved varying pH conditions within the same run. A constant glucose feed rate of 0.262 g L⁻¹ h⁻¹ was selected and pH varied from pH

4, with increments of 0.5 until pH 7. The starting pH of 4 was selected as it had been previously determined to be the optimum pH for FA production (Swart, Ronoh, *et al.*, 2022). The production phase was conducted for around 477 h, as a test for how long the cells could remain viable. After reaching pH 7, the NaOH dosing line was switched off and the pH allowed to naturally drop back to 4. The slow variations in pH were intended to simulate the pH conditions in the shake flask experiments.

For the last test on the hydration of FA to MA, pH 4 and pH 7 conditions were selected. In the first 72 h of production, the run was conducted at pH 4 and at a constant glucose feed rate of $0.329 \text{ g L}^{-1} \text{ h}^{-1}$. The nitrogen feed rate was $0.625 \text{ mg L}^{-1} \text{ h}^{-1}$. The above conditions were selected as they had been previously established to be the optimum for homofumarate production, corresponding to the highest FA yield reported in the literature with *R. delemar* (Swart, Ronoh, *et al.*, 2022). After 72 h, the pH was then increased to 7, and the glucose feed switched to zero. The nitrogen feed was decreased to $0.0625 \text{ mg L}^{-1} \text{ h}^{-1}$, corresponding to one tenth of the nitrogen previously fed into the reactor. Anaerobic conditions were induced by switching off the gas mixture used previously, consisting of 8% CO₂, with 18.4% O₂, and purging only CO₂ into the reactor.

3.2 Sample Preparation

The use of calcium carbonate as a neutralising agent presents a number of problems, including high broth viscosity (which is detrimental to equipment) and increased downstream costs. This is not only because calcium carbonate is insoluble, but also the use of calcium carbonate results in the formation of calcium malate and calcium fumarate, which have relatively low solubility. The following sample preparation procedure was used to dissolve the precipitated organic acids: 1 mL of a well-mixed culture broth was mixed with 1 mL of 1 M HCl and 18 mL of distilled water. The mixture was incubated at 80 °C for 20 min and vortexed several times during the incubation time. An aliquot was transferred to a 1.5 mL test tube and centrifuged for 5 min at $20,000 \times g$ in a desktop centrifuge. The clear supernatant was directly used for HPLC analysis.

3.3 Analytical Methods

Liquid samples (1 mL) were collected every 1 h using a single-channel pipette with replaceable pipette tips that were autoclaved at 121 °C for 20 min to avoid any contaminations in the cultivation media. pH measurements in the shake flask cultivations were not possible mid-run, and were only recorded after the end of the cultivation period. The concentrations of glucose, ethanol and organic acids were determined by High Performance Liquid

Chromatography (HPLC). An Agilent 1260 Infinity HPLC (Agilent Technologies, USA, equipped with an RI detector and a 300 mm \times 7.8 mm Aminex HPX-87H ion exchange column (Bio-Rad Laboratories, USA), was used. Two mobile phases were used for two methods of analysis. The first method made use of a 5 mM H₂SO₄ mobile phase solution fed at a flow rate of 0.6 mL min⁻¹, while the second method utilised a 20 mM H₂SO₄ mobile phase at the same flow rate. The second method resulted in the separation of the glucose, phosphate, and pyruvic acid peaks, thereby improving the accuracy of the glucose readings. The standard curves for the compounds were generated by plotting the area under the resulting peaks against known concentration values and thereafter fitting a straight line through the origin and at least two other known points. Table 2 below shows the standard concentration and the coefficient of determination (R²) values for each compound. HPLC standard calibration curves are shown in Appendix D.

Table 2: HPLC standard calibration: Concentration and coefficient of determination (R²) values for Glucose, malate, fumarate, glycerol, and ethanol.

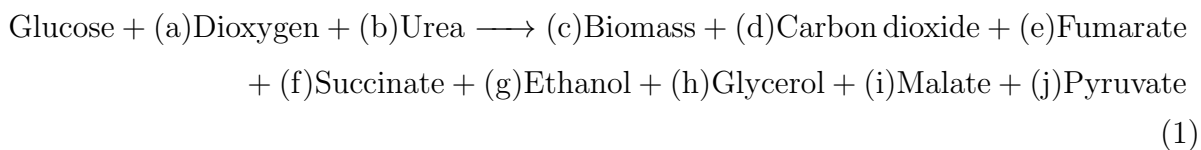
Compound	Conc. (g L ⁻¹)	R ²
Glucose	0.100950	1.00000
	1.00900	
	10.09500	
	50.01900	
Fumarate	0.199790	0.99992
	1.99800	
	9.99000	
Malate	0.109900	0.99991
	1.09900	
	10.99000	
Glycerol	0.100900	0.99988
	1.00900	
	10.09000	
Ethanol	0.100000	0.99996
	1.00000	
	10.00000	

Outlet gas composition (CO₂ and O₂) was measured using a tandem gas analyser (Magellan Biotech, UK). The concentration of metal ions in the fermentation cultures was determined using Inductively-Coupled Plasma – Optical Emission Spectrometry (ICP-OES) (ARCOS FHS12, Spectro Analytical Instruments, Kleve, Germany), utilising argon

as the carrier gas. Deionised water prepared in our laboratory was used in all aqueous preparations. The ICP calibration standards were obtained from Monitoring and Control Laboratories, South Africa. For the sample preparation, 1 mL of the well mixed sample was diluted 200^{-1} times to reduce the calcium ion concentrations to within the detection limits of the instrument. The diluted samples were then vortexed to ensure sufficient mixing, and transferred into 10 mL centrifuge tubes for testing. A sieve analysis was carried out using a nest of Labotec test sieves arranged in decreasing size from top to bottom (size ranging from 0.075 to 2 mm) (Midrand, South Africa). This was used to determine the particle size distribution of the insoluble solids. Cell morphology was examined using a Zeiss stereo discovery microscope (Zeiss, Germany).

3.4 Mass Balance

A black box model based on the metabolic map for *R. delemar* provided and discussed by Naude & Nicol (2017) was mathematically described through a mass balance over the system with the total chemical equation (Equation 1) below. Initial amounts of components from the growth run were accounted for using HPLC-determined time-zero sample concentrations in every production run. The biomass formula used was $\text{CH}_{1.8}\text{O}_{0.5}\text{N}_{0.2}$ (Nielsen & Villadsen, 1994), and tests were conducted where the initial and final biomass measurements were taken to quantify biomass growth during production.



Balances were done for C, N, and Degree of Reduction (DOR). In addition, all the HPLC determined values and biomass measurements were used to fully specify the system. The unknowns were predicted by solving the equation at every sampling point, and with data normalization, showing the carbon distribution over the cultivation period. The CO_2 determined from Equation 1 only represented carbon dioxide produced from the fermentation, and did not include the contribution from the dissolution of CaCO_3 .

4 Results and discussion

4.1 Biomass

Cell morphology plays a critical role in both free-cell and immobilised fermentations in achieving significant organic acid titres and low medium viscosity (Zhang, Yu, *et al*, 2015). For shake flask fermentations, small pellets (≈ 1 mm or less), have been found to be ideal. Therefore, controlling the fungal morphology was considered an important first step, with temperature, pH, agitation speed, and growth duration highlighted as key variables. After multiple iterations, nearly perfectly spherical pellets of diameter 0.9 mm were achieved with temperature, pH, agitation speed, and growth duration as follows: 34 °C, 5, 200 RPM, and 24 h (Figure 6a). These pellets were used for all the subsequent shake flask fermentations.

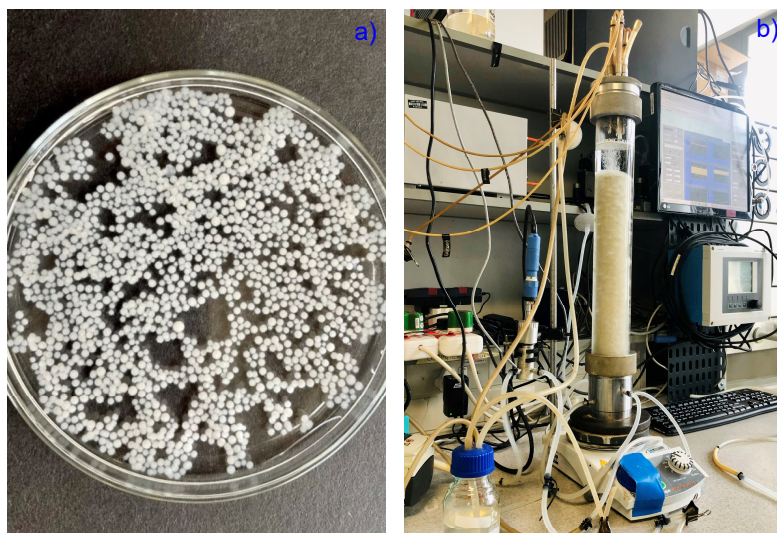


Figure 6: Cell morphology of *R. delemar* at the end of growth phase in (a) shake flask cultivations and (b) immobilised reactor cultivations. Pellets in shake-flask seed cultures were incubated at 34 °C, pH 5, 200 RPM and 24h growth duration resulting in pellets with 0.9 mm diameter. The growth phase in the immobilised reactor was conducted at pH 5 and 35°C. The biofilm that resulted had a thickness of ~ 1 mm.

In the immobilised reactor, growth media consisting of high glucose and urea concentrations were used during the growth phase, which typically lasted about 24 h. The growth phases for all runs were conducted at pH 5. Immobilisation of the biomass was achieved through the use of a polypropylene tube. Morphology control was achieved through adjusting parameters such as initial glucose and spore concentrations as described by Naude

(Naude & Nicol, 2017). The biofilm that resulted had a thickness of ~ 1 mm (Figure 6b).

4.2 Effect of CaCO_3 addition

To investigate the effect of the addition of CaCO_3 on the relative production of FA and MA, three different CaCO_3 concentrations were studied in 250 mL unbaffled Erlenmeyer flasks. The baseline amount of CaCO_3 was selected as 20 g L^{-1} and the fermentation conducted in triplicate. All fermentations had an initial substrate (glucose) concentration of around 100 g L^{-1} . Studies have shown that *R. delemar* has the ability to withstand high product and D-Glucose concentrations in excess of 100 g L^{-1} (Meussen *et al*, 2012). After 192 h, approximately 93.4% of the glucose was consumed, with the main products being fumarate and ethanol, as shown in Figure 7a. These results confirm the findings of Swart, Le Roux, *et al* (2020), indicating that *R. delemar* is indeed a Crabtree-positive organism, where the respiratory capacity reaches a maximum under excess glucose supply, resulting in the formation of ethanol under aerobic conditions as a metabolic overflow product.

The concentration of fumaric acid steadily increased throughout the fermentation period, reaching a value of $28.27 \pm 1.45 \text{ g L}^{-1}$, which corresponds to a yield of 0.28 g g^{-1} on glucose. Malic acid was first observed in HPLC sample analysis after 50 h of cultivation, and the concentration ($3.94 \pm 0.23 \text{ g L}^{-1}$) remained fairly constant thereafter (Figure 7a). Though one order of magnitude less than fumaric acid titres, the amount of MA produced was still significantly higher than the rest of the minor components.

During the last 30 h of the fermentation, a sharp decrease in ethanol concentration was observed. This is in tandem with the lowest glucose concentrations in the flasks, indicating the possibility that ethanol is being consumed as a substrate. *R. delemar* has the ability to grow under a wide range of carbon sources, including ethanol, as earlier established (Meussen *et al*, 2012). Therefore, ethanol can be broken down in the TCA cycle to produce more ATP (energy). The pH measured at the end of the fermentation was 4.17 ± 0.21 , a large drop from the initial pH recorded at the start of the fermentation (6.5 ± 0.1).

It was also observed that the fermentation broth became clear towards the end of the cultivation period, signalling a depletion of the CaCO_3 . This was an indication that more acid was formed than could be neutralised by the 20 g L^{-1} CaCO_3 in the fermentation broth.

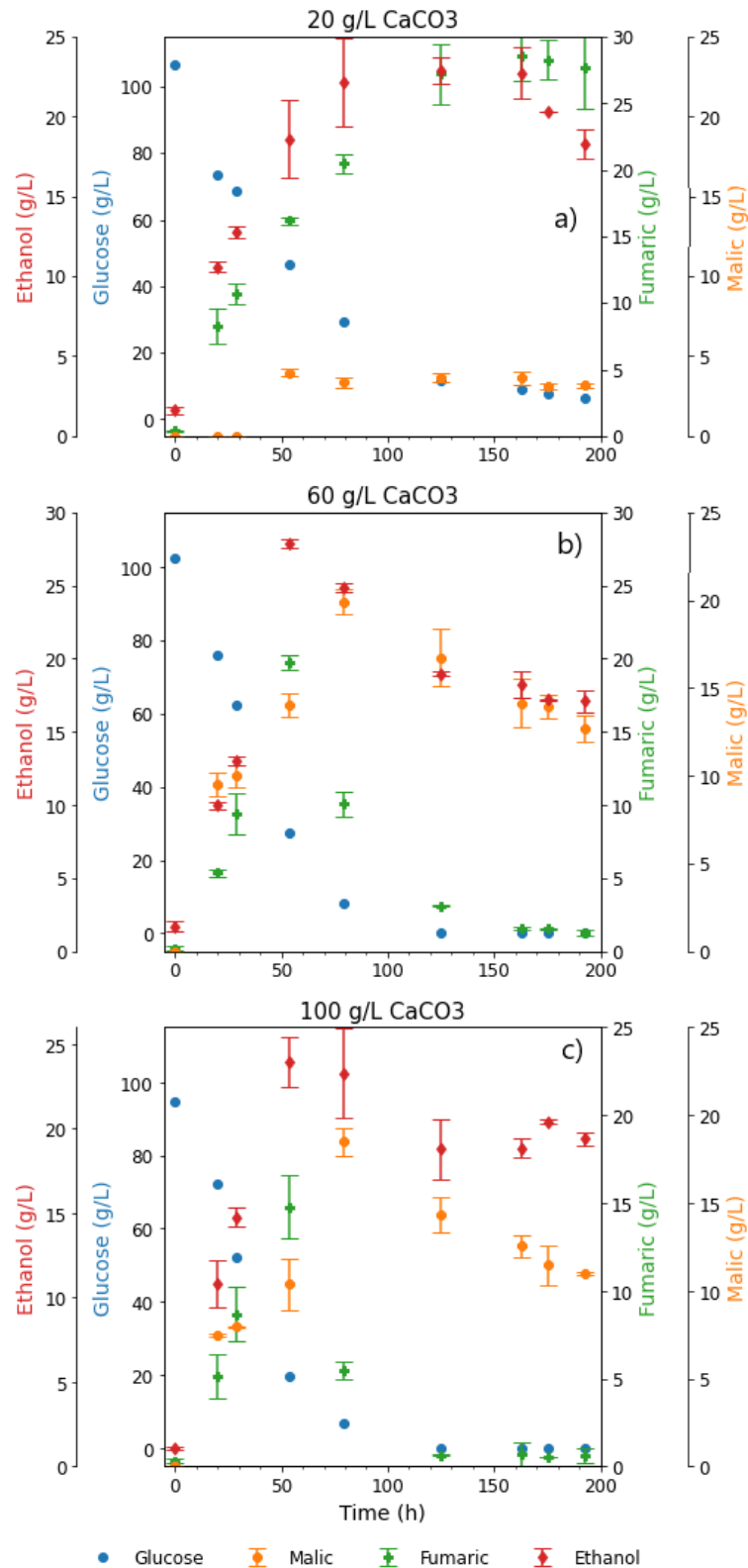


Figure 7: Extracellular concentrations of glucose and metabolites during shake flask cultivation of *R. delemar* on 100 g L⁻¹ glucose, in the presence of (a) 20 g L⁻¹ CaCO₃, (b) 60 g L⁻¹ CaCO₃, and (c) 100 g L⁻¹ CaCO₃. Cultures were incubated at 34 °C and 200 RPM. Results are the mean of triplicate experiments and error bars indicate the standard deviation.

To determine the amount of CaCO_3 that was required to fully neutralise the total acids produced, a calculation was done based on the neutralisation reactions, with the highest HPLC-determined concentrations of acids produced during the fermentation (fumarate, malate, pyruvate, and succinate). The amount of CaCO_3 required was determined to be 30.17 g L^{-1} .

It is also critical to highlight that a variation in the amount of H^+ would result in differences in the amounts of alkali required to control the pH. This is because the acids present may either be as fully dissociated, aqueous undissociated, or solid undissociated acid forms (Swart, Ronoh, *et al*, 2022). The stoichiometry of organic acid production and accompanying H^+ production as a function of pH at standard ambient temperature was previously presented by Taymaz-Nikerel *et al* (2013). The implication here is that the amount of alkali required to neutralise the acids produced towards the end of the fermentation would have been significantly less due to the drop in pH. The calculated amount of theoretical CaCO_3 required was based on the assumption of fully dissociated forms of all acids produced (pH 7 and higher). This means that, due to the gradual pH drop, the calculated amount of CaCO_3 required (30.17 g L^{-1}) was likely an overestimation of the actual amount.

A three-fold increase in the amount of CaCO_3 added was tested to ensure sufficient pH control for the duration of the fermentation, and to further elucidate the effect of increased amounts of CaCO_3 beyond the required amounts for neutralisation of the acids produced. The utilisation of 60 g L^{-1} CaCO_3 resulted in the first evidence of the co-production of FA and MA in almost equivalent amounts. This occurred within the first 55 h of the fermentation, with the highest FA and MA titres recorded as 19.77 g L^{-1} at 55 h and 19.91 g L^{-1} at 75 h, respectively. Thereafter, a significant drop in FA concentration was observed, resulting in a final fumarate concentration of 1.29 g L^{-1} by the end of the fermentation, as can be observed in Figure 7b. Given that *R. delemar* is predominantly a fumaric acid producer, the co-production of FA and MA, followed by the drop in FA concentration, were highlighted as key findings that would require further investigation. Interestingly, the MA and ethanol concentrations dropped towards the end of the fermentation once glucose was depleted, indicating the reassimilation of these as alternative substrates. The pH recorded at the end of the fermentation was 7.4, a slight increase from the initial pH recorded at the start of the fermentation. This is attributed to the sufficient presence of CaCO_3 in the fermentation broth.

The concentration profiles in the fermentations mediated with 100 g L^{-1} CaCO_3 (Figure 7c) were very similar to the 60 g L^{-1} CaCO_3 fermentation (Figure 7b). An initial rapid increase in fumarate concentration was observed, reaching a maximum of $14.79 \pm 1.83 \text{ g L}^{-1}$, and thereafter dropping to $0.93 \pm 0.33 \text{ g L}^{-1}$ by the end of the fermentation. The high-

est MA concentration was also recorded 80 h into the fermentation ($18.47 \pm 0.81 \text{ g L}^{-1}$), corresponding to a yield of 0.21 g g^{-1} .

The slight drop in malate and ethanol after the glucose was depleted was also akin to the previous CaCO_3 concentration tested. The increase in CaCO_3 concentration to 100 g L^{-1} did not translate into any significant variations in the metabolites produced or the glucose consumption rate, an indication that the fermentation conditions that resulted in the co-production of FA and MA, and the subsequent FA depletion, were maintained. In this case, again, the reassimilation of ethanol and MA was observed towards the end of the fermentation. The pH measured at the end of the fermentation was 7.37 ± 0.06 . The similarity in the final pH recorded in 60 and 100 g L^{-1} CaCO_3 fermentations provided a basis for further investigation of the effect of pH. It was observed from the carbon distribution shown in Figure 8, that there was a steady increase in the CO_2 across all fermentation conditions, an indication of increasing energy requirements towards the end of the fermentations. The increased energy demands was attributed to cell maintenance (an energy intensive procedure), and increased transport costs from the cell into the medium as the fermentation progressed.

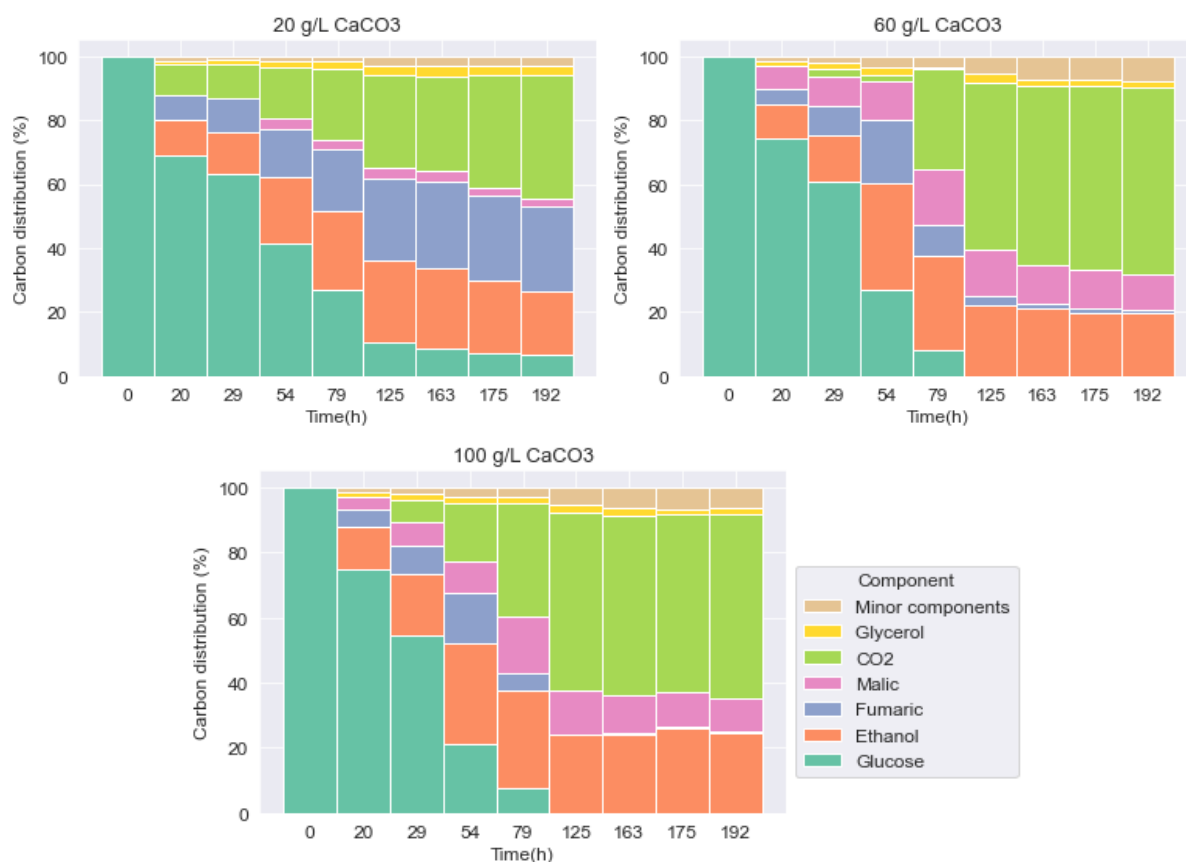


Figure 8: Metabolite distribution of *Rhizopus delemar* with the minor components including biomass, succinic acid and pyruvic acid

Besides increased CO₂ availability, the addition of CaCO₃ beyond the 20 g L⁻¹ baseline amount effectively implies the following changes in the fermentation broth that could influence the metabolites that *R. delemar* produces: increased presence of insoluble solids, increased Ca²⁺ concentrations, and increased pH. These factors were used as the departure point for the experimental design to determine the cause of the two phenomena: co-production of FA and MA, and the subsequent drop in fumaric acid concentrations.

4.3 Effect of Insoluble Solids: Comparison with MgCO₃

A similar experimental procedure was followed as outlined in the previous section, with the only variable being the alkali added. The MgCO₃ mass concentrations tested were also similar (20, 60, and 100 g L⁻¹) for ease of comparison of the resultant data. Magnesium carbonate offers many of the aforementioned benefits accrued from the use of calcium carbonate: (i) ‘all at once’ addition due to its insolubility (Gangl *et al*, 1990); (ii) increased concentrations of CO₂ (Zelle *et al*, 2010), and (iii) the formation of insoluble magnesium precipitates.

However, the pH values recorded at the end of the MgCO₃ fermentations were always slightly higher than their CaCO₃ counterparts, as indicated in Table 3. This can be attributed to the higher amount of carbonate (mole basis) present with the addition of similar mass-based amounts of MgCO₃ compared to CaCO₃. Moreover, while eliminating the presence of calcium ions, the addition of magnesium carbonate consequentially results in increased Mg²⁺ (Table 3), which would likely play a role in the metabolite distribution that results (Song *et al*, 2011). The main point of comparison in these experiments is the similar mass-based amounts of alkali added, therefore providing a basis to establish a preliminary test to investigate the influence of insoluble solids on the relative production of FA and MA.

Table 3: Inductively coupled plasma (ICP) measurements of Ca^{2+} and Mg^{2+} at the end of each production phase (198 h), in comparison to the baseline amount.

Run	C_x (g L^{-1})	Ca^{2+} (g L^{-1})	Mg^{2+} (g L^{-1})	pH
CaCO_3	20	4.79 ± 0.07	0.29 ± 0.01	4.17 ± 0.21
	60	5.63 ± 0.11	0.28 ± 0.01	7.45 ± 0.07
	100	5.69 ± 0.71	0.29 ± 0.02	7.37 ± 0.06
MgCO_3	20	0.74 ± 0.02	3.21 ± 0.05	4.6
	60	0.78 ± 0.02	6.54 ± 0.23	8.0
	100	0.78 ± 0.01	8.05 ± 0.16	8.1
Plaster sand	40	4.70 ± 0.07	0.31 ± 0.03	3.73 ± 0.06
	80	4.69 ± 0.71	0.29 ± 0.02	3.63 ± 0.06
	120	4.51 ± 0.60	0.29 ± 0.01	3.87 ± 0.12

With all experimental conditions kept constant, $20 \text{ g L}^{-1} \text{ MgCO}_3$ was first tested as the baseline amount of alkali in the shake flask cultivation of *R. delemar*. Two different regimes are mapped out in Figure 9, showing the co-production regime 1, and the fumarate depletion regime 2. The MgCO_3 -mediated fermentations are plotted alongside their CaCO_3 counterparts for ease of comparison of the two alkali. In the fermentation with $20 \text{ g L}^{-1} \text{ MgCO}_3$, all of the glucose was consumed in less than 100 h, much faster than in the fermentation with CaCO_3 . In contrast, for the fermentation with $60 \text{ g L}^{-1} \text{ MgCO}_3$, approximately 87% of the substrate was consumed in the same duration (100 h) and approximately 97% during the entire fermentation. The decrease in the glucose consumption rate was further exacerbated with the addition of more MgCO_3 , with only 84.2% of glucose being consumed by the end of the fermentation in the flask with $100 \text{ g L}^{-1} \text{ MgCO}_3$ (Figure 9). This is the reverse of the response that was observed in the fermentations with CaCO_3 , an indication of the likely effect of increased magnesium ion concentrations and pH (Table 3).

Fairly similar profiles were achieved for FA and MA in fermentations with $20 \text{ g L}^{-1} \text{ CaCO}_3$ and MgCO_3 . The only notable differences observed were the relatively high amount of MA that was initially produced in the MgCO_3 fermentation (12.69 g L^{-1}), and the slight tapering of FA concentrations toward the end of the fermentation. pH measurements taken at the end of the fermentation showed that there was a drop in pH to 4.6, also an indication of the insufficiency of the $20 \text{ g L}^{-1} \text{ MgCO}_3$ in meeting the pH control requirements in the fermentation (Table 3).

In the fermentations with 60 g L^{-1} alkali, the MA concentration profiles followed remarkably similar trends, a clear indicator that the co-production conditions highlighted in regime 1 were maintained across the fermentations with the two alkali. Fumarate concentrations in the fermentations with MgCO_3 were slightly lower than with CaCO_3 . This is attributed to the increased presence of magnesium ions in the fermentation broth. In a study on the expression and characterisation of *fumR* from *R. delemar*, Song *et al* (2011) found the slight inhibition of *fumR* activity with Mg^{2+} , and a small stimulatory effect with Ca^{2+} (further details in the next section). However, despite the lower concentration profile, the drop in fumarate concentrations in regime 2 was clearly visible for fermentations with both alkali. The pH recorded at the end of the fermentation in the 60 g L^{-1} MgCO_3 fermentation was 8, slightly higher than the final pH measured in its CaCO_3 counterpart. These findings were further corroborated in the fermentation with 100 g L^{-1} MgCO_3 , where a maximum MA concentration of 33.29 g L^{-1} was achieved, corresponding to a yield of 0.58 g g^{-1} and productivity of $0.35 \text{ g L}^{-1} \text{ h}^{-1}$. This was the highest MA concentration recorded in all the runs. A final pH of 8.1 was measured at the end of the run.

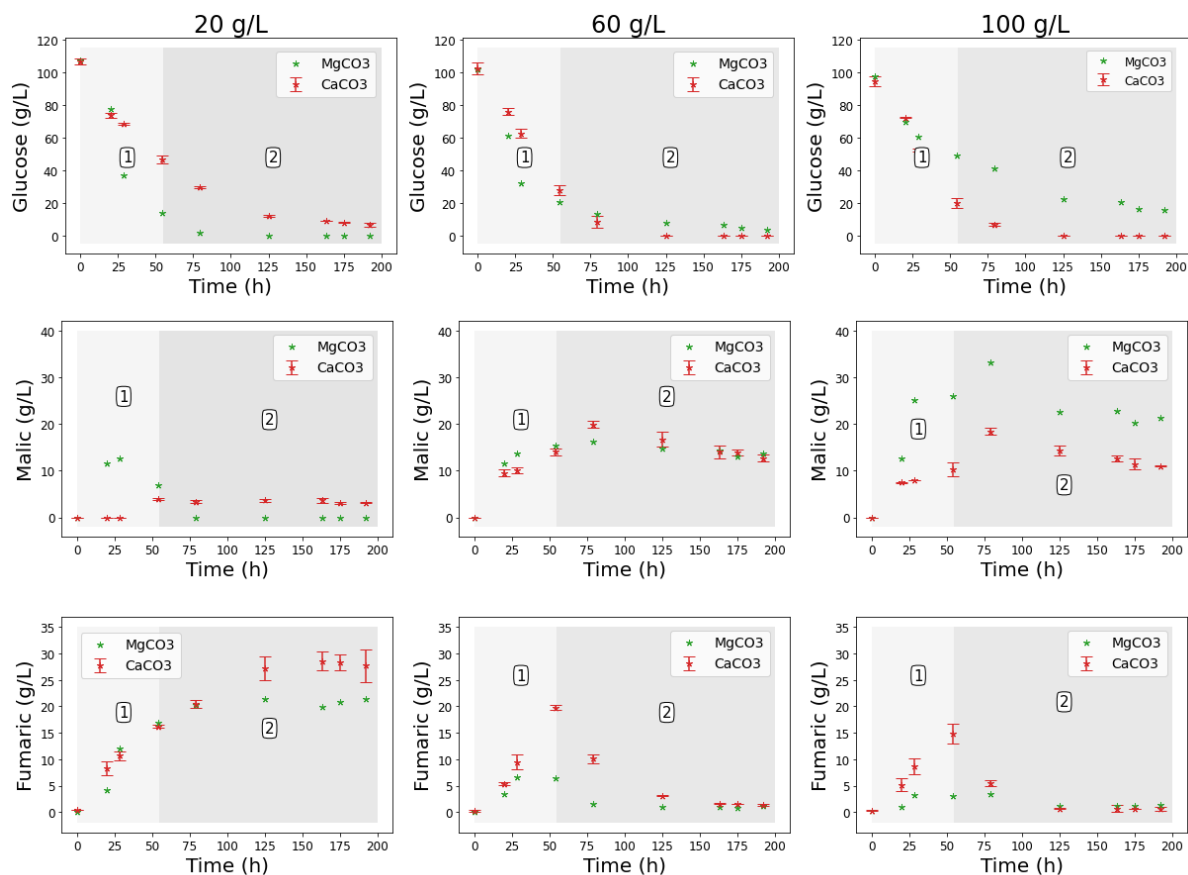


Figure 9: Comparison between the glucose, FA and MA profiles in shake flask cultivations with CaCO_3 and MgCO_3 concentrations varied between with 20 and 100 g L^{-1} . Regimes 1 and 2 indicate the co-production and fumarate depletion phases respectively.

The similarity in the profiles observed in the CaCO_3 and MgCO_3 fermentations (Figure 9) indicates a correlation between malic acid production and the increased presence of insoluble solids in the broth. However, there seems to be an underlying pH effect as the pH trends were fairly similar across the two runs. Moreover, there was an effect associated with the different metal ions present. To further elucidate the role of insoluble solids, the next test was conducted with plaster sand (PS) to simulate the presence of insoluble solids while eliminating the pH and metal ion effect, as discussed in the next section.

4.4 Effect of Insoluble Solids: Plaster Sand

The choice of plaster sand to simulate the conditions in the fermentation broth with CaCO_3 and MgCO_3 buffered cultures was based on the presumption that it contained no significant amounts of metal ions (Ca^{2+} and Mg^{2+}). The advantage of using PS was that not only would it provide a particle size similar to the CaCO_3 and MgCO_3 used in the previous section, but that it would also prevent the effects associated with metal ions and pH variations, thus allowing us to neatly test the effects of insoluble solids separately.

A sieve analysis was conducted to compare the particle size distribution of plaster sand and CaCO_3 . The results indicated that the plaster sand used was well graded, with a relatively even distribution of particles, as $\sim 80\%$ of particles lay within the range between 0.15 and 1.4 mm. CaCO_3 , on the other hand, displayed a slightly smaller particle size distribution, with over 90% of the particles falling within the range of 0.3 to 1.4 mm. However, the distributions were considered fairly comparable and thus plaster sand was used as an inert alternative to CaCO_3 and MgCO_3 . ICP measurements of the fermentation broth confirmed that increased amounts of plaster sand did not result in the increased presence of metal ions, an indication that the leaching of metal ions did not occur (Table 3).

Given the need for pH control, a baseline amount of 20 g L^{-1} CaCO_3 was initially added to all PS runs. Final pH measurements recorded were quite similar ($\sim \text{pH } 3.9$), an indication of comparable pH conditions throughout the different PS fermentations. The fermentation broth with PS became progressively thicker with increasing concentrations of insoluble solids. In the flasks with 120 g L^{-1} plaster sand, the pellets were suspended in the high-viscosity media, with minimal movement even under gyratory motion.

At the end of the run, the pellets were observed using a stereo microscope and the plaster sand-covered pellets appeared much larger in size (approximately 3.9 mm in diameter), as shown in Figure 10. This shows that the increase in PS concentrations, at least on a physical level, might have caused significant changes to the fermentation broth, which

would result in a physiological response—specifically, the co-production of fumaric and malic acids (regime 1) or the depletion of fumaric acid (regime 2). As aforementioned, *R. delemar* is a zygomycetes fungi that thrives in soils and dead organic matter. The main question thus was whether the high-viscosity broth significantly simulated its natural environment, triggering the response in regime 1 or 2.

The hypothesis is based on the thermodynamics research work by Tewari *et al* (1986), where they found that the $\Delta G_0'$ of the conversion of L-malic acid to fumaric acid is 3.6 kJ mol^{-1} , indicating that, at equilibrium, the L-malic acid concentration is higher than the fumaric acid concentration. The question of why *R. delemar* accumulates fumaric acid instead of malic acid can be attributed to a dicarboxylic acid transporter with a high selectivity for the former rather than the latter (Meussen *et al*, 2012). In principle, the addition of plaster sand at such high concentrations could result in a change in the selectivity bias of the transporter, based on the significant change in the environment in the broth. In its natural environment, *R. delemar* has been known to secrete acids in order to dissolve some of the solids in its immediate environment, and therefore malate selectivity by the transporter could be the way to achieve this. The chelating properties of malic acid in conjunction with the solubility of most metal compounds at low pH would thus be advantageous to the fungi in the poorly soluble fermentation broth conditions.



Figure 10: *R. delemar* pellets at the end of the plaster sand run. The pellets were collected from the flask that contained $20 \text{ g L}^{-1} \text{ CaCO}_3$ for pH control and 120 g L^{-1} plaster sand

An increase in PS concentrations, however, appeared to have no effect on glucose consumption, with complete depletion occurring 125 h into the production phase, as shown in Figure 11a. Fumarate concentrations also remained quite similar across all PS concentrations, and the characteristic drop in fumarate concentrations in regime 2 was absent (Figure 11b). Additionally, co-production of fumaric and malic acid did not occur in regime 1, as the MA concentrations remained fairly constant throughout the fermentation ($\sim 4 \text{ g L}^{-1}$), the observed similarity notwithstanding a three-fold increase in PS concentrations and a visible change in broth viscosity, as well as pellet size. This nullifies the hypothesis that insoluble solids had an effect on the response earlier observed (either regime 1 or regime 2).

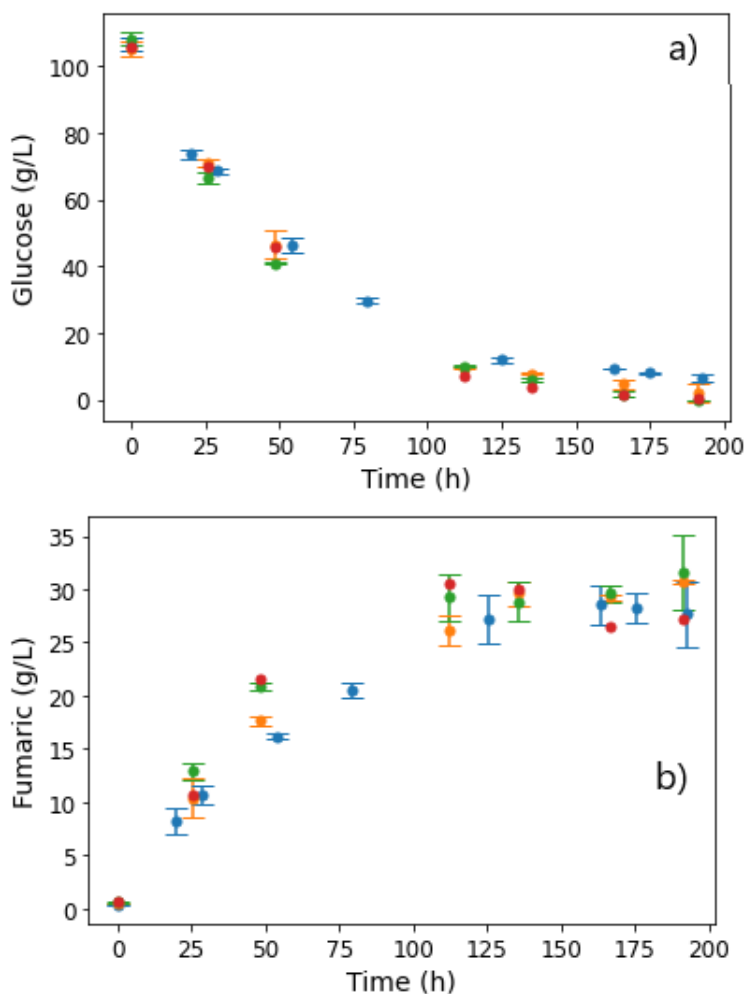


Figure 11: *Cont.*

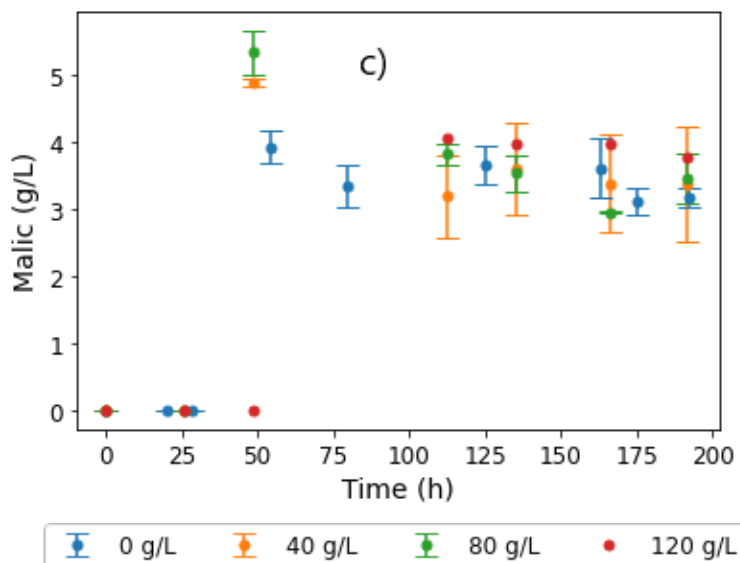


Figure 11: Extracellular concentrations of (a) glucose, (b) fumaric acid, and (c) malic acid during shake flask cultivation of *R. delemar* with different PS concentrations. Results are the mean of triplicate experiments and error bars indicate the standard deviation.

In the results from fermentations with PS (Figure 11), all four conditions resulted in the production of FA as the main organic acid ($\sim 30 \text{ g L}^{-1}$), and similar concentration profiles of all side products (Figure 16). With each condition conducted in triplicate, these results confirmed the repeatability of the experiments. The implication from these results is that the response from the CaCO_3 and MgCO_3 fermentations (regime 1 and 2) was likely to have been influenced by metal ions or pH, and not by insoluble solids. Given that no leaching of metal ions occurred in the runs with PS (see Table 3), the next set of experiments were conducted to extract the influence of Ca^{2+} on the two regimes.

4.5 Effect of calcium ions

As previously established, the use of CaCO_3 results in higher Ca^{2+} concentrations (Zelle *et al.*, 2010). Comparison between CaCO_3 and MgCO_3 indicated some similarities in the responses. Given that the presence of insoluble solids has been ruled out as a potential cause, the next set of experiments were conducted to extract the effect of Ca^{2+} on the two regimes. Experiments were conducted in a similar structure as the previous run, with 20 g L^{-1} CaCO_3 as the baseline amount (for pH control), to which additional calcium ion concentrations were added (in the form of CaCl_2).

It is well established that malate dehydrogenase (MDH), an enzyme located in the cytoplasm, converts oxaloacetate to L-malic acid, which is hydrated (reversibly) to fumaric

acid by the enzyme fumarase (FUM) (Meussen *et al*, 2012). Friedberg *et al* (1995) postulated that the reason behind the accumulation of fumaric acid by *R. delemar* is that a unique FUM induced under acid production conditions would produce fumaric acid, and the reverse reaction would be inhibited by increased amounts of fumaric acid (above 2 mmol L^{-1}). FUM is believed to be encoded by a single gene *fumR*, and it catalyses the reversible dehydration of L-malic acid to fumaric acid. Zhang, Yang, *et al* (2012) attempted to increase fumaric acid production by overexpressing *fumR*. However, their findings showed that overexpressing *fumR* increased FUM activities in both reaction directions, resulting in unusually high malic acid yields. Song *et al* (2011), in a study on the expression and characterisation of *fumR* from *R. delemar*, found a slight stimulatory effect of *fumR* activity with Ca^{2+} .

For the calcium ion tests, additional amounts of $5, 10, \text{ and } 20\text{ g L}^{-1}\text{ Ca}^{2+}$ were added to the baseline of $20\text{ g L}^{-1}\text{ CaCO}_3$ (Figure 12). Glucose consumption showed no significant variations in the lower calcium ion concentrations. However, for the experiments with the additional 20 g L^{-1} calcium ions, a significant drop in the glucose consumption rate was observed, as shown in Figure 12a. Similarly, fumarate production was hampered at the highest calcium concentration tested, while similar amounts were produced at lower concentrations. Moreover, a lag in MA production resulted, with a significant increase in malate concentrations only recorded over 100 h into the fermentation. This indicated that excessive calcium concentrations had the reverse effect on *fumR* activity. A proportional increase in glycerol concentrations with increasing calcium ion concentration conditions was also observed (Figure 17), an indication that calcium ions are involved in signalling pathways and stress responses, thus resulting in the formation of unwanted byproducts (Taymaz-Nikerel *et al*, 2013; Zelle *et al*, 2010).

In Figure 12c, the MA profiles show an interesting trend, with the additional 5 and 10 g L^{-1} calcium ion concentrations resulting in double the MA titres of the baseline. This corroborates the fact that the response in regime 1 (co-production of FA and MA) likely occurs as a consequence of the increased calcium ion concentrations. This is in tandem with the findings by Song *et al* (2011) on the slight stimulatory effect of calcium ions on *fumR*, thus resulting in increased fumarase activity in both directions and, as a consequence, increased malate concentrations (Song *et al*, 2011).

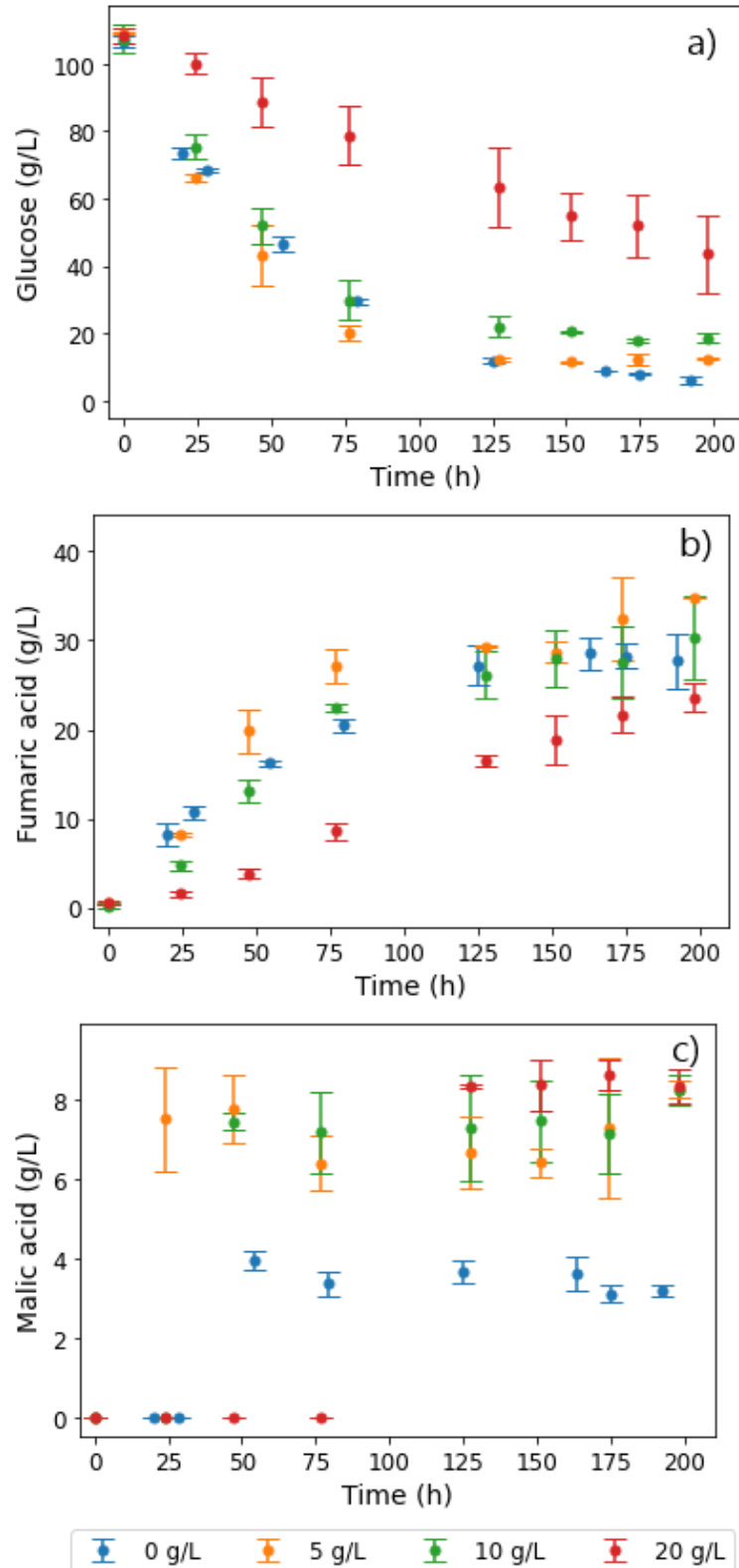


Figure 12: Extracellular concentrations of (a) glucose, (b) fumaric acid, and (c) malic acid during shake flask cultivation of *R.delemar* with different calcium ion concentrations. 20 g L^{-1} CaCO_3 was used for pH control as a baseline amount in these experiments and additional $5, 10$ and 20 g L^{-1} calcium ions were added onto the baseline in the form of CaCl_2 .

4.6 Effect of pH

4.6.1 Glucose Steps

Production of fumaric acid by *R. delemar* is typically performed at neutral pH values. CaCO_3 maintains the pH at around 6.5 in acid-forming microbial processes (Salek *et al.*, 2015). The use of neutralising agents not only contributes to a large portion of the production costs, but also leads to environmental waste (Y Liu *et al.*, 2015; Swart, Le Roux, *et al.*, 2020). Studies have shown that *R. delemar* is able to grow well at a wide temperature range (up to 40 °C) and pH range (4–9), an indication of its robust behaviour and wide application potential (Meussen *et al.*, 2012). There are some clear benefits in low-pH fermentation, including the formation of the undissociated form of fumaric acid, thus eliminating the need for neutralising agents, leading to simplified downstream processes and significantly lower costs (Y Liu *et al.*, 2015). However, given the increased production of malic acid with *R. delemar* in fermentations with CaCO_3 , investigating the role of pH in this response was considered critical.

The first set of experiments involved varying glucose feed rates between 0.131 and 0.329 g L⁻¹ h⁻¹ to investigate the effect of throttling glucose feed rates across four different pH conditions (4–7). Following a similar experimental procedure, Swart, Le Roux, *et al.* (2020) determined that *R. delemar* is a Crabtree-positive organism. This was then useful in discarding ethanol byproduct formation at a glucose feed rate of 0.197 g L⁻¹ h⁻¹ and at pH 5 (Swart, Ronoh, *et al.*, 2022). Further studies into the role of pH and urea addition on FA production compared three pH conditions (4, 5, and 6). The study found an optimum region for FA production at pH 4, a urea feed rate of 0.625 mg L⁻¹ h⁻¹, and a glucose feed rate of 0.329 g L⁻¹ h⁻¹. Moreover, pH 6 was found to be the least favourable condition with regard to FA production (Swart, Ronoh, *et al.*, 2022). This section of the research study was therefore considered additive, comparing the previously unstudied pH 7 condition to the other three (4, 5, and 6) (Swart, Ronoh, *et al.*, 2022), with a special focus on investigating the conditions that result in MA production.

The results in Figure 13a confirm the finding that higher-pH conditions were unfavourable for FA production with *R. delemar*. It can be seen that, compared to pH 4, 5, and 6, negligible amounts of FA were produced at pH 7. However, glucose accumulation did not occur until after around 80 h, an indication of the complete consumption of all glucose fed in this period (Figure 13d). The glucose consumed was mainly directed to MA and ethanol formation, both of which appeared early in the fermentation. Approximately 2.5 times more MA was formed than FA in the pH 7 fermentation, an indication of the drastic change in the response of the organism at pH 7 compared to pH 6.

However, it can be observed in Figure 13b that while relatively high amounts of MA were formed earlier in the fermentation in the pH 7 fermentation, MA production did not drastically increase further with an increase in glucose feed rates, but was instead similar to pH 6. This indicates that carbon was not channelled to MA production in replacement of FA production, therefore implying that a pH increment in conjunction with increased glucose feed rates has a moderate effect on MA production and a significant impact on FA production. Ethanol overflow, on the other hand, occurred right from the start of the fermentation, as seen in Figure 13c. This is in line with the trend of the ethanol overflow point occurring earlier, with increasing pH and glucose feed rates. This can be attributed to the relatively high osmotic and ionic stresses associated with the high pH, resulting in unwanted byproducts (Taymaz-Nikerel *et al*, 2013).

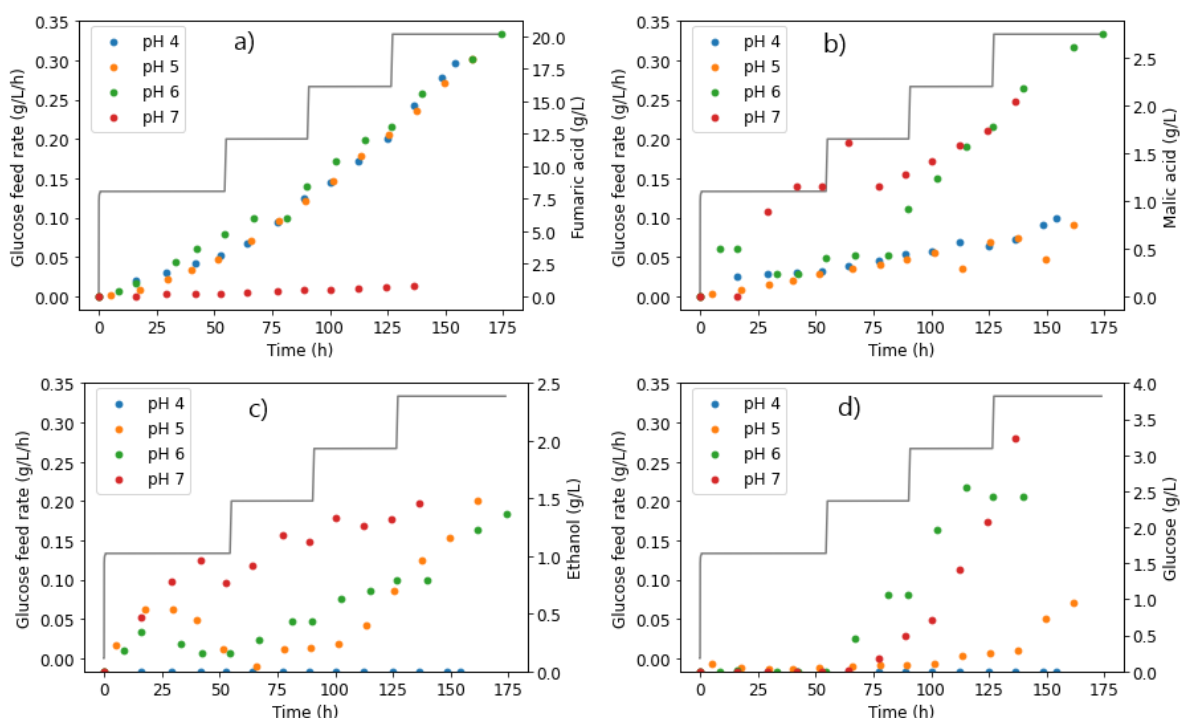


Figure 13: Glucose feed rates and extracellular concentrations of (a) fumaric acid, (b) malic acid, (c) ethanol, and (d) glucose, taken from the reactor during fermentation with *R.delemar* at different pH conditions

Glucose accumulation was only observed after the second glucose feed step ($0.197 \text{ g L}^{-1} \text{ h}^{-1}$), similar to the profile observed at pH 6, further establishing the finding that, at a higher pH, less glucose can be consumed (Swart, Ronoh, *et al*, 2022). This is clearly illustrated in contrast to the trends observed at lower pH values. In the pH 4 fermentation, there was complete consumption of all glucose at all glucose feed rates, whereas glucose accumulation only occurred at the highest glucose feed rate for the pH 5 fermentation. The implication here is that the inhibition of glucose consumption at higher-pH conditions would hinder the yields of metabolites that could be achieved, in comparison to the lower-pH conditions.

4.6.2 pH Steps

With the ability to control the pH precisely in the reactor, the pH was varied within the same run, from pH 4, with increments of 0.5 until pH 7. The starting pH of 4 was selected as it had been previously determined to be the optimum pH for FA production (Swart, Ronoh, *et al.*, 2022). Increasing the pH slowly up to 7 ensured a transition from optimal FA production conditions to more suboptimal conditions in the higher-pH conditions, simulating the slight pH increase in the shake flask cultivations owing to increased ethanol concentrations.

A constant glucose feed rate of $0.262 \text{ g L}^{-1} \text{ h}^{-1}$ and nitrogen feed rate of $0.625 \text{ mg L}^{-1} \text{ h}^{-1}$ were selected for this experiment. This would therefore allow for the investigation into the effect of gradual pH increase on the relative production of FA and MA. The production phase was much longer (477 h) as a test for how long the cells could remain viable. After reaching pH 7, the NaOH dosing was switched off and the pH allowed to naturally drop back to 4. This was to investigate whether the pH effects observed could be reversed with a subsequent drop in pH.

As shown in Figure 14a, fumarate was produced in relatively high amounts, with the final titre recorded as 65.89 g L^{-1} at the end of the run, corresponding to a yield of 0.527 g g^{-1} . This yield was significantly lower than that previously reported in the homofumarate production of FA at pH 4 (0.93 g g^{-1}), as a result of the inefficiency caused by the consistent pH increase throughout the run (Swart, Ronoh, *et al.*, 2022). Towards the end of the run, the FA production rate was observed to taper off but was not completely inhibited, as observed in the previous pH 7 only run; see Figure 14. This could be attributed to the slow increase in pH. Moreover, the tapering off of FA corresponds to the slight increase in MA production, with the latter reaching a final concentration of 6.28 g L^{-1} (Figure 14b). Glucose accumulation starts to occur also at this point. This provides an indication that the FA tapering off could be a result of the conversion of FA to MA. This has only been previously tested with *R. delemar* at specific conditions and with externally added FA (to be discussed in the next section) (Naude & Nicol, 2018).

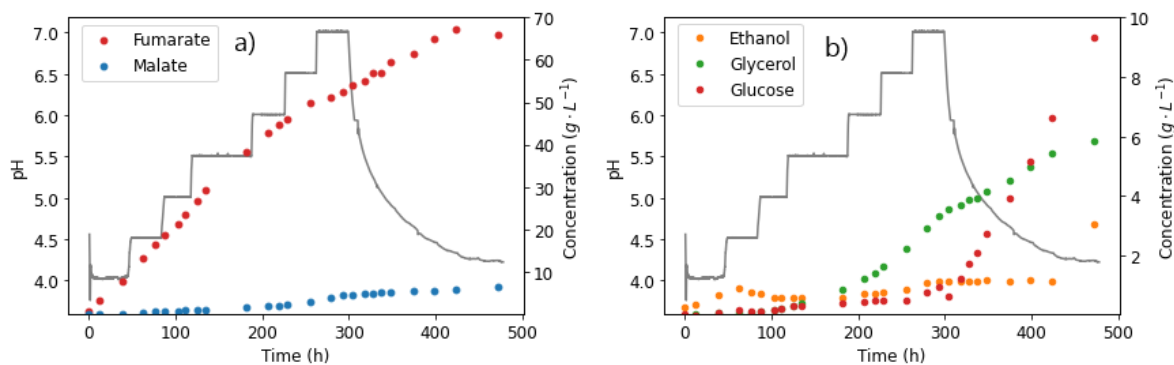


Figure 14: pH steps, and extracellular concentrations of (a) fumarate, (b) malate and ethanol taken from the reactor during fermentation with *R.delemar* at constant glucose feed rate of $0.262 \text{ g L}^{-1} \text{ h}^{-1}$

However, the occurrence of similar amounts of other side products such as glycerol and ethanol, as well as glucose accumulation indicate that this could be as a result of the inefficiencies of high pH conditions as observed in the previous glucose step tests. The duration of the run also played a role, given that fewer cells were likely viable towards the end of the run, resulting in inefficient glucose uptake. The results in this section however did not explain the characteristic drop in fumarate (observed earlier in regime 2). The next experiment was therefore carefully designed to investigate the in-situ hydration of FA to MA as a likely cause for response in regime 2.

4.6.3 Hydration of FA to MA

Naude & Nicol (2018), determined that three conditions were critical for the whole-cell hydration of FA to MA by *R. delemar*: (1) pH 7 or higher, (2) nitrogen starvation, and (3) complete glucose depletion. This neatly corresponds to the conditions in regime 2 that resulted in the characteristic drop in fumarate concentrations. In runs with both calcium carbonate and magnesium carbonate, all final pH conditions were measured as 7 or higher. Given that the runs were batch experiments, the limited amount of nitrogen present was likely completely depleted as the run progressed. Lastly, glucose starvation conditions were clearly present in regime 2, as most of the glucose had already been converted to fumarate and ethanol. Moreover, a significant amount of carbon was also channelled to respiration, based on a mass balance determination.

It was then postulated that the characteristic drop in fumarate concentrations was a result of whole-cell hydration to MA. This was considered a likely explanation as the drop in FA always corresponded to a further increase in MA concentrations. In the experiments with additional calcium ions, it was established that the co-production of

FA and MA (regime 1) was a result of increased calcium concentrations. However, as could be observed from the MA profiles (Figure 12c), there was an initial rise in MA concentration, which was then followed by a fairly constant MA profile for the rest of the cultivation period. The continued increase in MA concentration in regime 2 is then postulated to be not a result of increased calcium ion concentrations but, rather, the hydration of FA, resulting in the profiles observed.

In their study, Naude & Nicol (2018) determined the optimum conditions for the hydration of FA to MA, finding that, under aerobic conditions, a significant decrease in production half-life occurred. Moreover, the mass balance closure was only 95%, an indication that some of the FA had been channelled to respiration, decreasing the MA yield. In contrast, the study found that anaerobic conditions resulted not only in faster conversion, but also higher yields. However, their study utilised repeat batch experiments and externally added fumarate in the form of disodium fumarate. Therefore, to the best of our knowledge, the production of FA with *R. delemar*, followed by the in-situ hydration of FA to MA, has not been previously achieved. An experiment was then designed to attempt this, in order to prove the postulate that the depletion of FA in regime 2 was a result of the hydration of FA to MA.

To test this, pH 4 and pH 7 conditions were selected. In the first 72 h of production, the run was conducted at pH 4, a constant glucose feed rate of $0.329 \text{ g L}^{-1} \text{ h}^{-1}$, and a nitrogen feed rate of $0.625 \text{ mg L}^{-1} \text{ h}^{-1}$. The above condition was selected as it has been previously established to be the optimum for homofumarate production, corresponding to the highest FA yield reported in the literature with *R. delemar* (Swart, Ronoh, *et al.*, 2022). Moreover, this condition also provided an opportunity to exclusively and productively form FA, which was subsequently used for the next phase. Lastly, the fact that no glucose accumulation occurred at this condition was an advantage, as the glucose fed into the reactor could immediately be switched off, quickly ushering in glucose starvation conditions, a critical requirement for the hydration of FA to occur.

After 72 h, approximately 14.71 g L^{-1} FA and negligible amounts of MA had been produced (Figure 15a). The pH was then increased to 7, and the glucose feed switched to zero. The nitrogen feed was decreased to $0.625 \text{ mg L}^{-1} \text{ h}^{-1}$, corresponding to one tenth of the nitrogen previously fed into the reactor. Anaerobic conditions were induced by switching off the gas mixture used previously, consisting of 8% CO_2 , with 18.4% O_2 , and purging only CO_2 into the reactor. Figure 15 shows the metabolite profiles achieved.

The characteristic drop in fumarate concentrations was observed, while MA titres rapidly increased, as shown in Figure 15a. After 101 h, the FA concentration had dropped to 9.19 g L^{-1} , and MA had increased to 5.09 g L^{-1} . Given the glucose starvation conditions

in the reactor, the sudden increase in MA concentrations and the corresponding depletion of FA could only be attributed to the hydration of FA to MA. The run was stopped after 112 h, with the final FA and MA concentrations recorded as 4.61 g L^{-1} and 8.20 g L^{-1} , respectively. A slight increase in ethanol concentrations was observed after the switch to anaerobic conditions. This was an indication that some of the FA was being used to meet the energy requirements, albeit inefficiently due to the anaerobic conditions, thus resulting in the formation of ethanol.

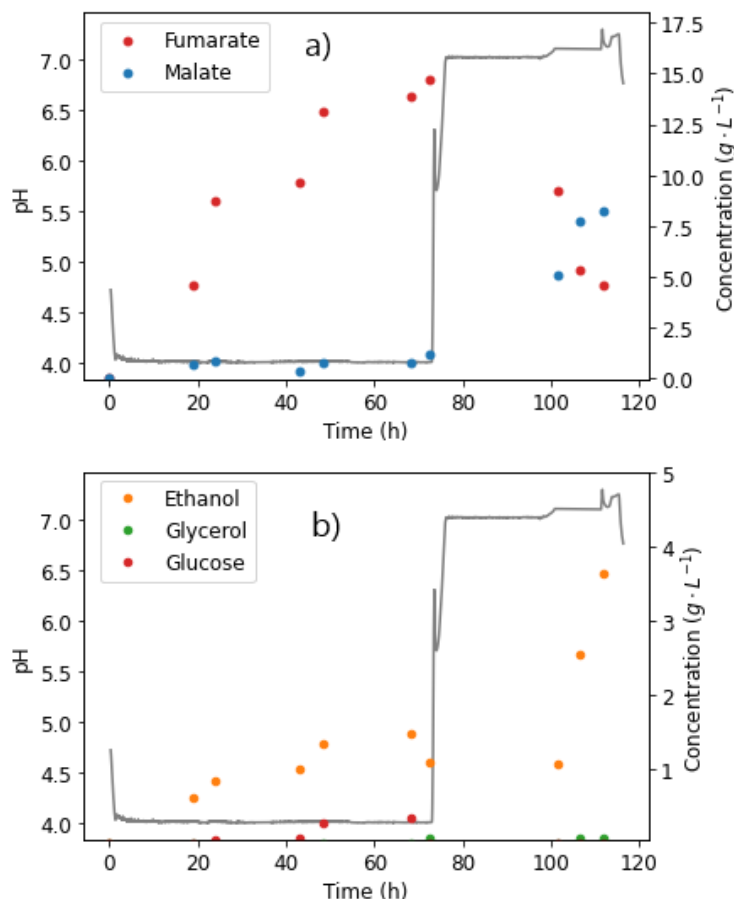


Figure 15: pH steps, and extracellular concentrations of (a) fumarate, malate and (b) side products taken from the reactor during fermentation with *R.deleamar* at constant glucose feed rate of $0.329 \text{ g L}^{-1} \text{ h}^{-1}$. After 72 h, the glucose feed was switched to zero, pH increased to 7, and nitrogen feed decreased to $0.0625 \text{ mg L}^{-1} \text{ h}^{-1}$. Anaerobic conditions were also induced in this phase.

It can be seen from a comparison of the FA and MA concentrations achieved in this study, in contrast to the titres and productivities previously reported in the literature and shown in Table 4, that fumaric acid production with *R. deleamar* has been well developed and optimised. However, it is clear that there is significant potential for malic acid production with *R. deleamar*, drawing on the insights from the effect of calcium ions and the hydration of FA.

Table 4: Comparison of fumaric acid and malic acid production using *R. delemar*.

Process	Fumaric Acid			Malic Acid		
	Titre (g L ⁻¹)	Productivity (g L ⁻¹ h ⁻¹)	Titre (g L ⁻¹)	Productivity (g L ⁻¹ h ⁻¹)	Titre (g L ⁻¹)	Productivity (g L ⁻¹ h ⁻¹)
Immobilised reactor [†]	65.89	0.138	8.20	0.205		
Immobilised reactor (Swart, Ronoh, <i>et al.</i> , 2022)	-	0.305	-	-		
Immobilised reactor (Gu <i>et al.</i> , 2013)	32.03	1.33	-	-		
Immobilised reactor (Naude & Nicol, 2017)	40.13	0.32	2.6	0.022		
Stirred tank (YQ Fu <i>et al.</i> , 2010)	56.2	0.7	-	-		
Stirred tank (Xu <i>et al.</i> , 2012)	41.1	0.37	-	-		
Shake flask [†]	34.84	0.176	33.29	0.168		
Shake flask (Martin-Dominguez, Bouzas-Santiso, <i>et al.</i> , 2020)	30	-	25	-		
Shake flask (H Liu <i>et al.</i> , 2017)	46.7	-	-	-		
Shake flask (Zhang, Yu & Yang, 2015)	50.2	0.34	2.1	0.015		

[†] Current Study. The species names are dissimilar in some of the published reports, but all of the strains are classified as *R. oryzae* (the previous name of the reclassified *R. delemar*) according to the American Type Culture Collection (ATCC) catalogue.

This experiment provided a clear proof of concept—an indication that the drop in fumarate concentrations in regime 2 was a result of the hydration of FA. Moreover, this finding completes the picture of the response in regime 2, explaining the further increase in MA concentrations as well as the depletion of FA. The implication, therefore, is that the responses from the two regimes were a consequence of the following: increased calcium ions initiated the co-production of FA and MA (regime 1). The high initial glucose concentrations in the shake flask cultivations resulted in the maximum respiratory capacity of *R. delemar* being exceeded and, as a consequence, the production of ethanol in significant quantities. As the fermentation progressed, a slight increase in pH occurred due to increased carbonate concentrations in the fermentation broth. With the onset of glucose and nitrogen starvation conditions, all the requirements for the hydration of FA to MA were attained (regime 2).

5 Conclusion and recommendations

pH plays a critical role in microbial cultures as it directly affects the homeostasis of the microbe due to changes in acid dissociation, enzyme activities, equilibrium conditions, diffusion of nutrients into and out of the microbes and the efficiency of energy producing mechanisms. Calcium carbonate has been used extensively in shake flask fermentations due to its ability to offer continuous neutralisation, a consequence of its poor solubility. By varying calcium carbonate concentrations in shaker flask experiments of *R. delemar*, two clear regimes were observed: the co-production of FA and MA, and subsequently, the depletion of FA. The co-production of FA and MA was conclusively linked to increased calcium ion concentrations, a factor of increased presence of CaCO_3 . However, the sustained increase in MA concentrations in regime 2, as FA concentrations dropped, could not be attributed to calcium ions. It was determined that increased concentrations of insoluble solids neither had an effect on glucose consumption nor the relative production of FA and MA. An underlying pH trend was observed in the shake flask fermentations. By carefully increasing the pH in a continuous flow reactor of *R. delemar*, the reason for the drop in FA concentrations was uncovered as the hydration of FA to MA, which occurs at pH 7 (or higher), and at glucose and nitrogen starvation conditions.

These observations were validated in a continuous flow system in which 10.1 g L^{-1} of in situ produced FA (at pH 4) was hydrated to 7.41 g L^{-1} MA (at pH 7). This study provides the first known evidence for in situ whole cell generation of FA and subsequent hydration of FA to MA by *R. delemar* in a single reactor system. Constitutively, the findings presented in this study provides a relatively simple approach for the sustainable production of malic acid from *R. delemar*.

The work presented in this research was exploratory in nature and therefore provides the basis for further optimisation work in future. One such optimisation opportunity lies in the investigation into the effect of nitrogen on FA production and the subsequent hydration step to MA. While numerous studies have been conducted in a bid to determine the optimum urea feed rate for maximal fumaric acid production with *R. delemar*, the extent of the role that nitrogen plays in the hydration of FA to MA is yet to be fully described. Reactor operation is also another area that shows great promise. As a prominent facultative anaerobe, *R. delemar* can function aerobically or anaerobically, with the former linked to high FA yields and titres. Anaerobic conditions on the other hand were found to significantly improve the hydration process. There is therefore room to optimise the switch from aerobic conditions to anaerobic conditions in the in situ whole cell generation of FA and the subsequent hydration process, with special attention given to eliminating ethanol production thus increasing the conversion efficiency.

Additionally, a study on the determination of the optimum temperature for the hydration step could also result in a significant increase in MA yields and titres.

References

Abe, A, Oda, Y, Asano, K and Sone, T (2007) “*Rhizopus delemar* is the proper name for *Rhizopus oryzae* fumaric-malic acid producers” *Mycologia*, 99, (5): 714–722 ISSN: 00275514 DOI: 10.3852/mycologia.99.5.714.

Abe, A, Sone, T, Sujaya, N, Saito, K, Oda, Y, Asano, K and Tomita, F (2003) “Rdna ITS Sequence of *Rhizopus oryzae*: Its application to classification and identification of lactic acid producers” *Bioscience, Biotechnology and Biochemistry*, 67,(8): 1725–1731 ISSN: 13476947 DOI: 10.1271/bbb.67.1725.

Agency, GE (2019) *Feedstocks for the chemical industry* tech. rep.: pp. 2–3 URL: https://www.dena.de/fileadmin/dena/Publikationen/PDFs/2019/Feedstocks_for_the_chemical_industry.

Beauchemin, KA and McGinn, SM (June 2006) “Methane emissions from beef cattle: Effects of fumaric acid, essential oil, and canola oil” *Journal of Animal Science*, 84, (6): 1489–1496 ISSN: 0021-8812 DOI: 10.2527/2006.8461489x.

Beauprez, JJ, De Mey, M and Soetaert, WK (2010) “Microbial succinic acid production: Natural versus metabolic engineered producers” *Process Biochemistry*, 45, (7): 1103–1114 ISSN: 13595113 DOI: 10.1016/j.procbio.2010.03.035.

Cao, N (1997) “Production of fumaric acid by immobilized rhizopus using rotary biofilm contactor” *Applied Biochemistry and Biotechnology - Part A Enzyme Engineering and Biotechnology*, 63-65, (1): 387–394 ISSN: 02732289 DOI: 10.1007/BF02920440.

Cao, N, Du, J, Gong, CS and Tsao, GT (1996) “Simultaneous Production and Recovery of Fumaric Acid from Immobilized *Rhizopus oryzae* with a Rotary Biofilm Contactor and an Adsorption Column” 62, (8): 2926–2931 DOI: 10.1128/aem.62.8.2926–2931.1996.

Chi, Z, Wang, Zp, Wang, Gy, Khan, I and Chi, Zm (2016) “Microbial biosynthesis and secretion of l-malic acid and its applications” 8551, (5): 99–107 DOI: 10.3109/07388551.2014.924474.

Dai, Z, Zhou, H, Zhang, S, Gu, H, Yang, Q, Zhang, W, Dong, W, Ma, J, Fang, Y, Jiang, M and Xin, F (2018) “Current advance in biological production of malic acid using wild

type and metabolic engineered strains” *Bioresource Technology*, 258, (January): 345–353 ISSN: 18732976 DOI: 10.1016/j.biortech.2018.03.001.

Dinçer, İİ (2018) *Comprehensive Energy Systems*, English 1st ed. vol. 1 Elsevier, Amsterdam, Netherlands ISBN: 9780128149256 0128149256 0128095970 9780128095973 URL: <https://www.elsevier.com/books/comprehensive-energy-systems/dincer/978-0-12-809597-3>.

Ding, Y, Li, S, Dou, C, Yu, Y and He, H (2011) “Production of fumaric acid by *Rhizopus oryzae*: Role of carbon-nitrogen ratio” *Applied Biochemistry and Biotechnology*, 164, (8): 1461–1467 ISSN: 02732289 DOI: 10.1007/s12010-011-9226-y.

Fatih Birol (2020) *Key World Energy Statistics 2020* tech. rep. August: p. 4649 URL: <https://www.iea.org/reports/key-world-energy-statistics-2020>.

Ferreira, JA, Lennartsson, PR, Edebo, L and Taherzadeh, MJ (2013) “Zygomycetes-based biorefinery : Present status and future prospects”: pp. 1–40 ISBN: 4633435590 DOI: 10.1016/j.biortech.2012.09.064.

Foster, JW and Waksman, SA (1939) “The Production of Fumaric Acid by Molds Belonging to the Genus *Rhizopus*” *Journal of the American Chemical Society*, 61, (1): 127–135 ISSN: 0002-7863 DOI: 10.1021/ja01870a043.

Friedberg, D, Peleg, Y, Monsonogo, A, Maissi, S, Battat, E, Rokem, JS and Goldberg, I (1995) “The fumR gene encoding fumarase in the filamentous fungus *Rhizopus oryzae*: cloning, structure and expression” *Gene*, 163, (1): 139–144 ISSN: 03781119 DOI: 10.1016/0378-1119(95)00367-F.

Fu, YQ, Li, S, Chen, Y, Xu, Q, Huang, H and Sheng, XY (2010) “Enhancement of fumaric acid production by *Rhizopus oryzae* using a two-stage dissolved oxygen control strategy” *Applied Biochemistry and Biotechnology*, 162, (4): 1031–1038 ISSN: 02732289 DOI: 10.1007/s12010-009-8831-5.

Fu, YQ, Xu, Q, Li, S, Chen, Y and Huang, H (2010) “Strain improvement of *Rhizopus oryzae* for over-production of fumaric acid by reducing ethanol synthesis pathway” *Korean Journal of Chemical Engineering TA - TT* -, 27, (1): 183–186 ISSN: 0256-1115 DOI: 10.1007/s11814-009-0323-3.

Gangl, IC, Weigand, WA and Keller, FA (1990) “Economic comparison of calcium fumarate and sodium fumarate production by *Rhizopus arrhizus*” *Applied Biochemistry and Biotechnology*, 24-25, (1): 663–677 ISSN: 0273-2289 DOI: 10.1007/BF02920287.

Geyer, M, Onyancha, FM, Nicol, W and Brink, HG (2018) “Malic Acid Production by *Aspergillus Oryzae*: The Role of CaCO₃” *Chemical Engineering Transactions*, (July) DOI: 10.3303/CET1870301.

Goldberg, I, Rokem, JS and Pines, O (2006) “Organic acids: old metabolites, new themes” *Chemical Technology and Biotechnology*, 1611, (October 2005): 1601–1611 DOI: 10.1002/jctb.

Gu, C, Zhou, Y, Liu, L, Tan, T and Deng, L (2013) “Production of fumaric acid by immobilized *Rhizopus arrhizus* on net” *Bioresource Technology*, 131, 303–307 ISSN: 18732976 DOI: 10.1016/j.biortech.2012.12.148.

Huang, L, Wei, P, Zang, R, Xu, Z and Cen, P (2010) “High-throughput screening of high-yield colonies of *Rhizopus oryzae* for enhanced production of fumaric acid” *Annals of Microbiology*, 60, (2): 287–292 ISSN: 15904261 DOI: 10.1007/s13213-010-0039-y.

IEA (2020) *Energy Technology Perspectives 2020* tech. rep. DOI: 10.1787/ab43a9a5-en.

Jang, YS, Kim, B, Shin, JH, Choi, YJ, Choi, S, Song, CW, Lee, J, Park, HG and Lee, SY (2012) “Bio-based production of C2-C6 platform chemicals” *Biotechnology and Bioengineering*, 109, (10): 2437–2459 ISSN: 00063592 DOI: 10.1002/bit.24599.

Ji, XJ, Huang, H and Ouyang, PK (2011) “Microbial 2,3-butanediol production: A state-of-the-art review” *Biotechnology Advances*, 29, (3): 351–364 ISSN: 07349750 DOI: 10.1016/j.biotechadv.2011.01.007.

Jianxin, DU (1997) “Fumaric acid production in airlift loop reactor with porous sparger” *Applied Biochemistry and Biotechnology*, 63-65, (1): 541–556 ISSN: 02732289 DOI: 10.1007/bf02920452.

Jones, CS1 and Mayfield, S (2016) *Our energy future: introduction to renewable energy and biofuels*, English 1st ed. University of California Press, Oakland, California ISBN: 9780520964280 0520964284 DOI: 10.1525/9780520964280.

Jongh, NW de, Swart, RM and Nicol, W (2021) “Fed-batch growth of *Rhizopus oryzae*: Eliminating ethanol formation by controlling glucose addition” *Biochemical Engineering Journal*, 169, (February) ISSN: 1873295X DOI: 10.1016/j.bej.2021.107961.

Karaffa, L, Fekete, E and Kubicek, CP (2021) “The role of metal ions in fungal organic acid accumulation” *Microorganisms*, 9, (6): 1–13 ISSN: 20762607 DOI: 10.3390/microorganisms9061267.

Kenealy, W, Zaady, E and Du Preez, JC (1986) “Biochemical aspects of fumaric acid accumulation by *Rhizopus arrhizus*” *Applied and Environmental Microbiology*, 52, (1): 128–133 ISSN: 00992240 DOI: 10.1128/aem.52.1.128-133.1986.

Kikuchi, Y, Kanematsu, Y and Okubo, T (2016) “A computer-aided scenario analysis of national and regional energy systems based on feasible technology options”, in: *Computer Aided Chemical Engineering*, TA - TT -: pp. 1959–1964 ISBN: 978-0-444-63428-3 DOI: 10.1016/B978-0-444-63428-3.50331-3LK.

Kövilein, A, Kubisch, C, Cai, L and Ochsenreither, K (2019) “Malic acid production from renewables: a review” *Chemical Technology and Biotechnology*, (December) DOI: 10.1002/jctb.6269.

Kövilein, A, Umpfenbach, J and Ochsenreither, K (2021) “Biotechnology for Biofuels Acetate as substrate for l - malic acid production with *Aspergillus oryzae* DSM 1863” *Biotechnology for Biofuels*, 1–15 ISSN: 1754-6834 DOI: 10.1186/s13068-021-01901-5.

Lan, R and Kim, I (2018) “Effects of organic acid and medium chain fatty acid blends on the performance of sows and their piglets” *Animal Science Journal*, 89, (12): 1673–1679 ISSN: 1344-3941 DOI: <https://doi.org/10.1111/asj.13111>.

Layton, BE (2008) “A comparison of energy densities of prevalent energy sources in units of joules per cubic meter” *International Journal of Green Energy*, 5, (6): 438–455 ISSN: 15435075 DOI: 10.1080/15435070802498036.

Lebreton, L and Andrady, A (2019) “Future scenarios of global plastic waste generation and disposal” *Palgrave Communications*, 5, (1): 1–11 ISSN: 20551045 DOI: 10.1057/s41599-018-0212-7.

Lee, JW, Han, MS, Choi, S, Yi, J, Lee, TW and Lee, SY (2011) “Organic Acids: Succinic and Malic Acids”, in: Moo-Young, MBTCB(E (Ed.), Academic Press, Burlington:

pp. 149–161 ISBN: 978-0-08-088504-9 DOI: <https://doi.org/10.1016/B978-0-08-088504-9.00183-5>.

Li, X, Gu, X, Lai, C, Ouyang, J and Yong, Q (2016) “Production of Fumaric Acid by *Rhizopus oryzae* in Simultaneous Saccharification and Fermentation using Xylo-Oligosaccharides Manufacturing Waste Residue” *BioResources*, 11, (4): 8831–8843 ISSN: 19302126 DOI: 10.15376/biores.11.4.8831-8843.

Lin, CSK and Luque, R (2014) *Renewable resources for biorefineries LK*, English 1st ed. RSC green chemistry, 1757-7179 ; no. 27 Royal Society of Chemistry, Cambridge DOI: 10.1515/gps-2015-0008.

Liu, H, Hu, H, Jin, Y, Yue, X, Deng, L, Wang, F and Tan, T (June 2017) “Co-fermentation of a mixture of glucose and xylose to fumaric acid by *Rhizopus arrhizus* RH 7-13-9.” *eng Bioresource technology*, 233, 30–33 ISSN: 1873-2976 (Electronic) DOI: 10.1016/j.biortech.2017.02.035.

Liu, Y, Lv, C, Xu, Q, Li, S, Huang, H and Ouyang, P (2015) “Enhanced acid tolerance of *Rhizopus oryzae* during fumaric acid production” *Bioprocess and Biosystems Engineering*, 38, (2): 323–328 ISSN: 16157605 DOI: 10.1007/s00449-014-1272-8.

Lund, H (2007) “Renewable energy strategies for sustainable development” *Energy*, 32, (6): 912–919 ISSN: 0360-5442 DOI: <https://doi.org/10.1016/j.energy.2006.10.017>.

Machtelt, B, Robert, vdB, Mariët, vdW and Peter, P (2005) *A Top-Down Systems Biology Approach*, pp. 25–35 DOI: 10.1128/9781555816636.ch3.

Martin-Dominguez, V, Bouzas-Santiso, L, Martinez-Peinado, N, Santos, VE and Ladero, M (2020) “Kinetic modelling of the coproduction process of fumaric and malic acids by *Rhizopus arrhizus* NRRL 1526” *Processes*, 8, (2) ISSN: 22279717 DOI: 10.3390/pr8020188.

Martin-Dominguez, V, Estevez, J, De Borja Ojembarrena, F, Santos, VE and Ladero, M (2018) “Fumaric acid production: A biorefinery perspective” *Fermentation*, 4, (2) ISSN: 23115637 DOI: 10.3390/fermentation4020033.

McGinn, SM, Turner, D, Tomkins, N, Charmley, E, Bishop-Hurley, G and Chen, D (2011) “Methane Emissions from Grazing Cattle Using Point-Source Dispersion” *Journal of*

Environmental Quality TA - TT -, 40, (1): 22–27 ISSN: 0047-2425 DOI: 10.2134/jeq2010.0239LK-<https://UnivofPretoria.on.worldcat.org/oclc/8409071158>.

Merckel, RD (2014) “Fast and microwave-induced pyrolysis bio-oil from *Eucalyptus grandis*: Possibilities for upgrading” *mathesis*, South Africa: University of Pretoria URL: <http://hdl.handle.net/2263/43913>.

Meussen, BJ, De Graaff, LH, Sanders, JP and Weusthuis, RA (2012) “Metabolic engineering of *Rhizopus oryzae* for the production of platform chemicals” *Applied Microbiology and Biotechnology*, 94, (4): 875–886 ISSN: 01757598 DOI: 10.1007/s00253-012-4033-0.

Naude, A and Nicol, W (2017) “Fumaric acid fermentation with immobilised *Rhizopus oryzae*: Quantifying time-dependent variations in catabolic flux” *Process Biochemistry*, 56, (April 2018): 8–20 ISSN: 13595113 DOI: 10.1016/j.procbio.2017.02.027.

Naude, A and Nicol, W (2018) “Malic acid production through the whole-cell hydration of fumaric acid with immobilised *Rhizopus oryzae*” *Biochemical Engineering Journal*, 137, 152–161 ISSN: 1873295X DOI: 10.1016/j.bej.2018.05.022.

Ng, T, Hesser, R, Stieglitz, B, Griffiths, B and Ling, L (1986) “Production of tetrahydrofuran/1, 4 butanediol by a combined biological and chemical process” in: *Biotech Bioeng Symp* vol. 17: pp. 344–363 URL: <https://eurekamag.com/research/028/974/028974820.php>.

Nielsen, JH and Villadsen, J (1994) *Bioreaction engineering principles*, English Plenum Press, New York URL: <https://link.springer.com/book/10.1007/978-1-4419-9688-6>.

Overman, SA and Romano, AH (1969) “Pyruvate carboxylase of *Rhizopus nigricans* and its role in fumaric acid production” *Biochemical and Biophysical Research Communications*, 37, (3): 457–463 ISSN: 10902104 DOI: 10.1016/0006-291X(69)90937-1.

Patten, JD and Waldroup, PW (1988) “Use of Organic Acids in Broiler Diets” *Poultry Science*, 67, (8): 1178–1182 ISSN: 0032-5791 DOI: <https://doi.org/10.3382/ps.0671178>.

Peleg, Y, Battat, E, Scrutton, MC and Goldberg, I (1989) “Isoenzyme pattern and subcellular localisation of enzymes involved in fumaric acid accumulation by *Rhizopus oryzae*” *Applied Microbiology Biotechnology*, 334–339 DOI: 10.1007/BF00184985.

Rhodes, RA, Moyer, AJ, Smith, ML and Kelley, SE (1959) “Production of Fumaric Acid by *Rhizopus arrhizus*” *Applied Microbiology*, 7, (2): 74–80 ISSN: 0003-6919 DOI: 10.1128/am.7.2.74-80.1959.

Rhodes, RA, Lagoda, AA, Misenheimer, TJ, Smith, ML, Anderson, RF and Jackson, RW (1962) “Production of Fumaric Acid in 20-Liter Fermentors” *Applied Microbiology*, 10, (1): 9–15 ISSN: 0003-6919 DOI: 10.1128/aem.10.1.9-15.1962.

Roa Engel, CA (2010) “Integration of fermentation and cooling crystallisation to produce organic acids” Delft, Netherlands: pp. 1–161 URL: <http://resolver.tudelft.nl/uuid:0518e010-08f9-40c0-a731-e7edfe379c2d>.

Roa Engel, CA, Straathof, AJ, Zijlmans, TW, Van Gulik, WM and Van Der Wielen, LA (2008) “Fumaric acid production by fermentation” *Applied Microbiology and Biotechnology*, 78, (3): 379–389 ISSN: 01757598 DOI: 10.1007/s00253-007-1341-x.

Roa Engel, CA, Van Gulik, WM, Marang, L, Van der Wielen, LA and Straathof, AJ (2011) “Development of a low pH fermentation strategy for fumaric acid production by *Rhizopus oryzae*” *Enzyme and Microbial Technology*, 48, (1): 39–47 ISSN: 01410229 DOI: 10.1016/j.enzmictec.2010.09.001.

Rodrigue, JP, Comtois, C and Slack, B (2009) *The geography of transport systems*, English 5th ed. Routledge, London ISBN: 9780415483230 0415483239 9780415483247 0415483247 9780203884157 0203884159 URL: <https://transportgeography.org>.

Salek, SS, Turnhout, AG van, Kleerebezem, R and Loosdrecht, MC van (2015) “pH control in biological systems using calcium carbonate” *Biotechnology and Bioengineering*, 112, (5): 905–913 ISSN: 10970290 DOI: 10.1002/bit.25506.

Sebastian, J, Hegde, K, Kumar, P, Rouissi, T and Brar, SK (2019) “Bioproduction of fumaric acid: an insight into microbial strain improvement strategies” *Critical Reviews in Biotechnology*, 39, (6): 817–834 ISSN: 15497801 DOI: 10.1080/07388551.2019.1620677.

Skory, CD (2004) “Lactic acid production by *Rhizopus oryzae* transformants with modified lactate dehydrogenase activity” *Applied Microbiology and Biotechnology*, 64, (2): 237–242 ISSN: 01757598 DOI: 10.1007/s00253-003-1480-7.

Song, P, Li, S, Ding, Y, Xu, Q and Huang, H (2011) “Expression and characterization of fumarase (FUMR) from *Rhizopus oryzae*” *Fungal Biology*, 115, (1): 49–53 ISSN: 18786146 DOI: 10.1016/j.funbio.2010.10.003.

Swart, RM, Ronoh, DK, Brink, H and Nicol, W (2022) “Continuous Production of Fumaric Acid with Immobilised *Rhizopus oryzae*: The Role of pH and Urea Addition” *Catalysts*, 12, (1) DOI: 10.3390/catal12010082.

Swart, RM, Le Roux, F, Naude, A, De Jongh, NW and Nicol, W (2020) “Fumarate production with *Rhizopus oryzae*: Utilising the Crabtree effect to minimise ethanol by-product formation” *Biotechnology for Biofuels*, 13, (1): 1–10 ISSN: 17546834 DOI: 10.1186/s13068-020-1664-8.

Taymaz-Nikerel, H, Jamalzadeh, E, Borujeni, AE, Verheijen, PJ, Van Gulik, WM and Heijnen, SJ (2013) “A thermodynamic analysis of dicarboxylic acid production in microorganisms” *Biothermodynamics: The Role of Thermodynamics in Biochemical Engineering*, 547–579.

Tewari, Y, Gajewski, E, Goldberg, R and Rouissi, D (1986) “Thermodynamics of the conversion of aqueous L-Aspartic acid to fumaric acid and ammonia” *Biophysical Chemistry*, 24, (6): 13–23 DOI: 10.1016/0301-4622(86)85054-2.

Vanholme, B, Desmet, T, Ronsse, F, Rabaey, K, Van Breusegem, F, De Mey, M, Soetaert, W and Boerjan, W (2013) “Towards a carbon-negative sustainable bio-based economy” *Frontiers in Plant Science*, 4, ISSN: 1664-462X DOI: 10.3389/fpls.2013.00174.

Vassilev, N (1991) “Organic acid production by immobilized filamentous fungi” *Topics in Catalysis*, 5, (4): 188–190 ISSN: 0269915x DOI: 10.1016/S0269-915X(09)80484-9.

Werpy, T and Petersen, G (2004) “Top Value Added Chemicals from Biomass Volume I” *U.S. National Renewable Energy Laboratory*, Medium: ED, Size: 76 pp. pages DOI: 10.2172/15008859.

West, TP (2017) *Microbial Production of Malic Acid from Biofuel-Related Coproducts and Biomass*, vol. 3 2 DOI: 10.3390/fermentation3020014.

World Economic Forum (2016) *The new plastics economy: Rethinking the future of plastics* tech. rep. January: p. 120 eprint: /www.ellenmacarthurfoundation.org/publications

(http:) URL: <https://www.weforum.org/reports/the-new-plastics-economy-rethinking-the-future-of-plastics>.

Xu, G, Chen, X, Liu, L and Jiang, L (2013) “Fumaric acid production in *Saccharomyces cerevisiae* by simultaneous use of oxidative and reductive routes” *Bioresource Technology*, 148, 91–96 ISSN: 18732976 DOI: 10.1016/j.biortech.2013.08.115.

Xu, Li, Huang and Wen, J (2012) “Key technologies for the industrial production of fumaric acid by fermentation” *Biotechnology Advances*, 30, (6): 1685–1696 ISSN: 07349750 DOI: 10.1016/j.biotechadv.2012.08.007.

Xu, Q, Li, S, Fu, Y, Tai, C and Huang, H (2010) “Two-stage utilization of corn straw by *Rhizopus oryzae* for fumaric acid production” *Bioresource Technology*, 101, (15): 6262–6264 ISSN: 0960-8524 DOI: <https://doi.org/10.1016/j.biortech.2010.02.086> URL: <https://www.sciencedirect.com/science/article/pii/S0960852410003974>.

Zelle, RM, De Hulster, E, Kloezen, W, Pronk, JT and Van Maris, AJ (2010) “Key process conditions for production of C4 dicarboxylic acids in bioreactor Batch cultures of an engineered *saccharomyces cerevisiae* strain” *Applied and Environmental Microbiology*, 76, (3): 744–750 ISSN: 00992240 DOI: 10.1128/AEM.02396-09.

Zhang, K, Yang, ST, Chalmers, JJ and Wood, D (2012) “Fumaric Acid Fermentation by *Rhizopus oryzae* with Integrated Separation Technologies” Columbus, Ohio: pp. 1–230.

Zhang, K, Yu, C and Yang, ST (2015) “Effects of soybean meal hydrolysate as the nitrogen source on seed culture morphology and fumaric acid production by *Rhizopus oryzae*” *Process Biochemistry*, 50, (2): 173–179 ISSN: 13595113 DOI: 10.1016/j.procbio.2014.12.015.

Zhou, Du, J and Tsao (2002) “Comparison of fumaric acid production by *Rhizopus oryzae* using different neutralizing agents” *Bioprocess and Biosystems Engineering*, 25, (3): 179–181 ISSN: 16157591 DOI: 10.1007/s004490100224.

Zhou, Y (1999) “Fumaric acid fermentation by *Rhizopus oryzae* in submerged systems” English phdthesis, Ann Arbor, MI, USA: Purdue University: p. 149 ISBN: 978-0-493-28900-7 URL: <https://docs.lib.purdue.edu/dissertations/AAI3018471/>.

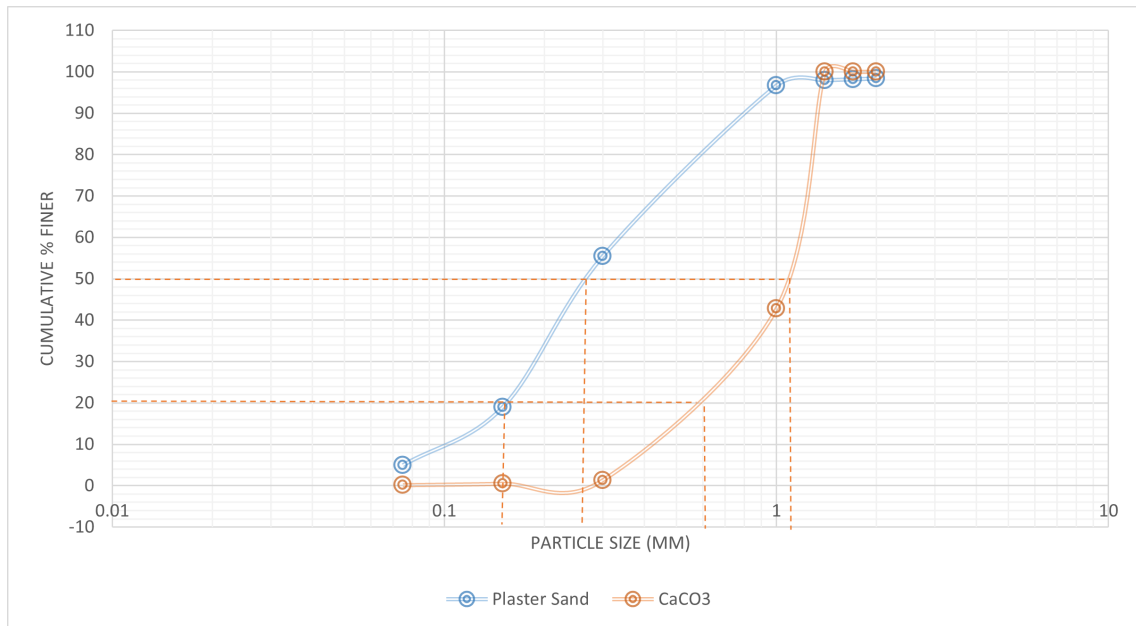
Zhou, Y, Du, J and Tsao, GT (2000) “Mycelial pellet formation by *Rhizopus oryzae* ATCC 20344” *Applied Biochemistry and Biotechnology - Part A Enzyme Engineering and Biotechnology*, 84-86, 779–789 ISSN: 02732289 DOI: 10.1385/abab:84-86:1-9:779.

Zhou, Z, Du, G, Hua, Z, Zhou, J and Chen, J (2011) “Optimization of fumaric acid production by *Rhizopus delemar* based on the morphology formation” *Bioresource Technology*, 102, (20): 9345–9349 ISSN: 09608524 DOI: 10.1016/j.biortech.2011.07.120.

Appendix A

Particle Size Distribution

Sieve Number	Sieve size (mm)	Sieve mass (g)	Mass total (g)	Mass retained (g)	% on each sieve	Cumulative percent retained $\sum R_n$	Percent Finer %
1	2	563.14	571.22	8.08	1.616	1.616	98.384
2	1.7	374.3	375.31	1.01	0.202	1.818	98.182
3	1.4	359.69	361.15	1.46	0.292	2.11	97.89
4	1	334.11	340.16	6.05	1.21	3.32	96.68
5	0.3	272.75	479.02	206.27	41.254	44.574	55.426
6	0.15	258.3	440.56	182.26	36.452	81.026	18.974
7	0.075	260.28	330.67	70.39	14.078	95.104	4.896
8		457.38	481.73	24.48	4.896	100	0
1	2	563.14	563.14	0	0	0	100
2	1.7	374.3	374.33	0.03	0.006	0.006	99.994
3	1.4	359.69	359.72	0.03	0.006	0.012	99.988
4	1	334.11	620.41	286.3	57.26	57.272	42.728
5	0.3	272.75	479.68	206.93	41.386	98.658	1.342
6	0.15	258.3	262.47	4.17	0.834	99.492	0.508
7	0.075	260.28	262.03	1.75	0.35	99.842	0.158
8		457.38	457.48	0.79	0.158	100	0



Appendix B

Glycerol profiles

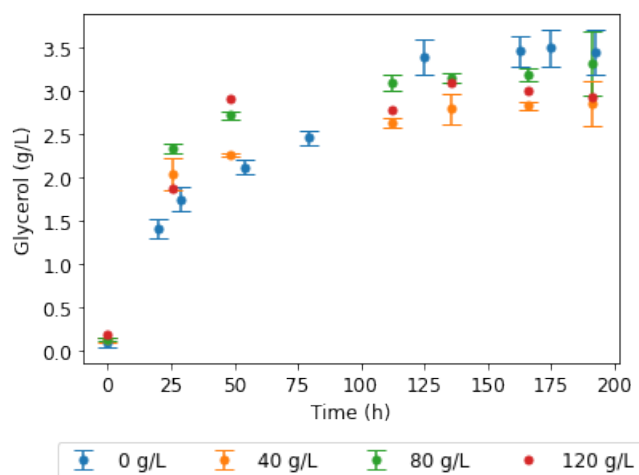


Figure 16: Extracellular concentrations of glycerol during shake flask cultivation of *R. delemar* with different plaster sand concentrations. Results are the mean of triplicate experiments and error bars indicate the standard deviation.

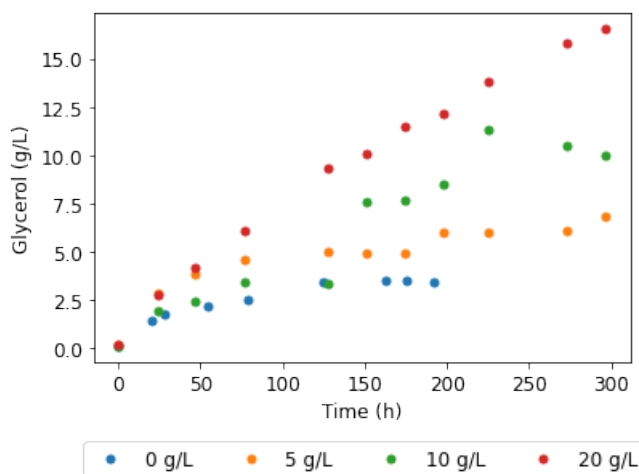


Figure 17: Extracellular concentrations of glycerol during shake flask cultivation of *R. delemar* with different calcium ion concentrations. $20 \text{ g L}^{-1} \text{ CaCO}_3$ was used for pH control as a baseline amount in these experiments and additional $5, 10$ and 20 g L^{-1} calcium ions were added onto the baseline in the form of CaCl_2 .

Appendix C

IEA License

List or description of CC-licensed Content

As referred to in the [Notice for CC-licensed Content](#) and the [IEA terms and conditions](#), the following IEA content constitutes "CC-licensed Content" and is licensed as set out in the [Notice for CC-licensed Content](#):

Name or description of CC-licensed Content	Applicable CC license
<p>All text, reports (including associated datasets, figures and infographics), articles, commentaries, standalone graphs, figures, and infographics produced by the IEA and featuring in the introduction and under the 'News', 'Latest' and 'Key Points' sections of the Russia's War on Ukraine webpages.</p> <p>Photographs are specifically excluded.</p>	<p>CC BY 4.0 International</p>

The following CC-licensed Content carries its own Creative Commons notice which will prevail over the terms set out in the Notice for CC-licensed Content to the extent of any inconsistency.

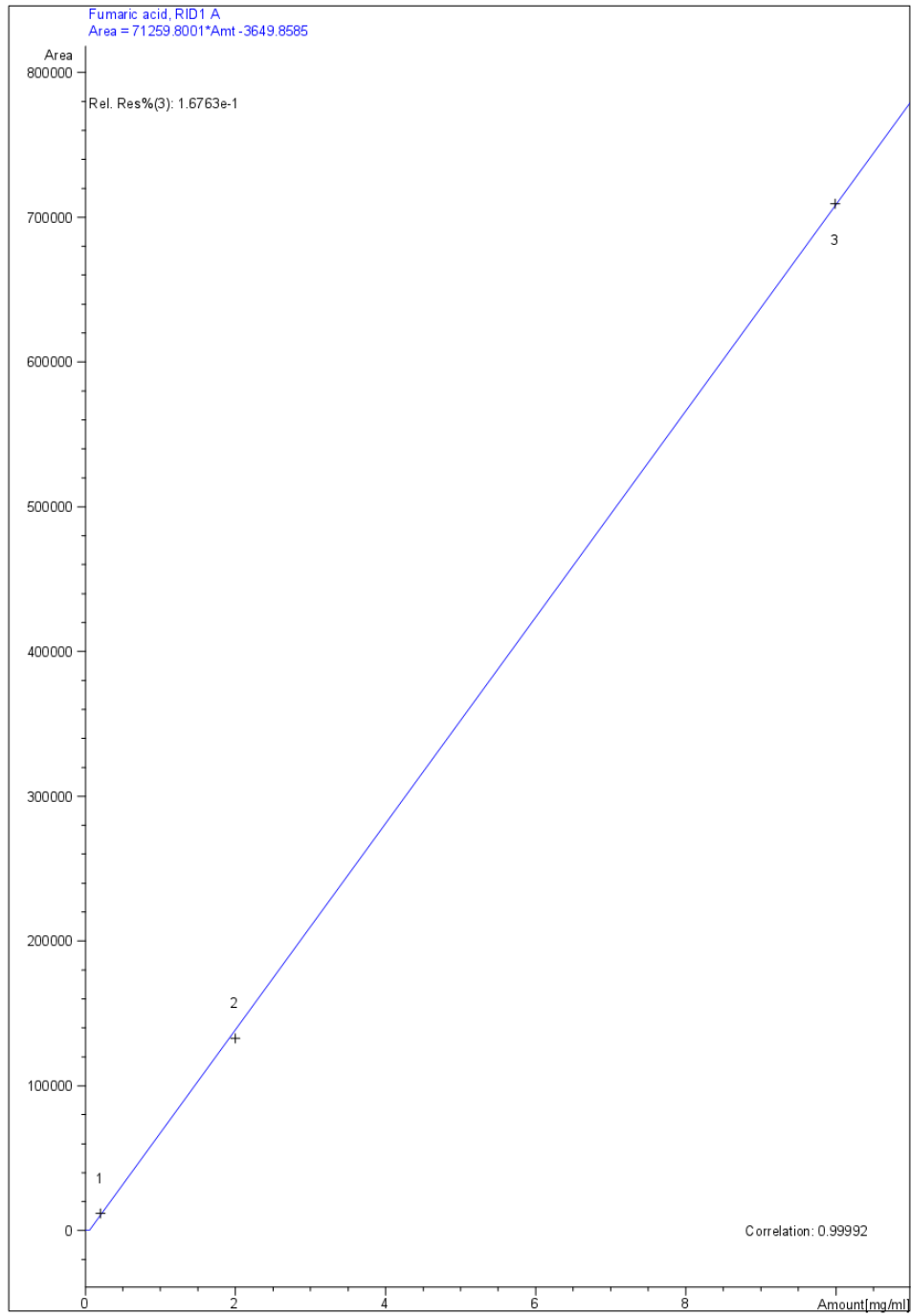
Name or description of CC-licensed Content	Applicable CC licence and notice
<p>Weather for Energy Tracker https://www.iea.org/articles/weather-for-energy-tracker</p>	 <p>This database is made available under the Creative Commons Attribution-NonCommercial-NoDerivatives 3.0 IGO license (CC BY-NC-ND 3.0 IGO) http://creativecommons.org/licenses/by-nc-nd/3.0/igo/deed.en, you are free to copy and redistribute the material, provided the use is for non-commercial purposes, under the following conditions:</p> <p>Attribution - Please cite the database as follows: IEA and CMCC (2022), <i>Weather for Energy Tracker</i>, License: Creative Commons CC BY-NC-ND 3.0 IGO</p> <p>Third-party content—The OECD/IEA and CMCC do not necessarily own each component of the content and data contained within this database. Therefore, neither the OECD, IEA nor CMCC warrant that the use of any such third-party owned individual component will not infringe on the rights of those third parties. The risk of claims resulting from such infringement rests solely with you. If you wish to re-use a component of the work in accordance with this CC BY-NC-ND 3.0 IGO license, it is your responsibility to determine whether permission is needed for that re-use and to obtain permission from the relevant copyright owner. Examples of components can include, but are not limited to, data, figures, or images.</p>
<p>Net Zero by 2050 dataset https://www.iea.org/data-and-statistics/data-product/net-zero-by-2050-scenario</p>	<p>This data is available under the Creative Commons Attribution-NonCommercial-ShareAlike 3.0 IGO license (CC BY-NC-SA 3.0 IGO) You are free to copy, redistribute and adapt the data, provided the use is for non-commercial purposes, under the following conditions:</p>

	<p>Third-party content - If you wish to use or re-disseminate any data in this file that is sourced or attributed to a third party, it is your responsibility to determine whether permission is needed for that re-use and to obtain permission from the relevant owner.</p> <p>Attribution - Please cite the IEA's data as follows: International Energy Agency (2021), <i>Net Zero by 2050</i>, IEA, Paris: Net Zero by 2050 Scenario - Data product - IEA. License: Creative Commons Attribution CC BY-NC-SA 3.0 IGO.</p> <p>Adaptations - If you create derived material based on IEA data, please use the following notice: Based on data from International Energy Agency (2021) <i>Net Zero by 2050: Net Zero by 2050 Scenario - Data product - IEA</i>; as modified by [insert your legal entity name].</p> <p>ShareAlike - If you transform, build on or otherwise modify the IEA's data in order to derive new material, you must distribute your derived material under the same license as the original.</p> <p>Commercial usage: If you wish to use the data for commercial purposes or use or distribute your derived material for commercial purposes then please refer to the related product "Net Zero by 2050 Scenario - Commercial usage".</p>
<p>Methane Tracker Database https://www.iea.org/articles/methane-tracker-database</p>	<p>This data is available under the Creative Commons Attribution 4.0 license (CC BY 4.0) You are free to copy, redistribute and adapt the data under the following conditions:</p> <p>Third-party content - If you wish to use or re-disseminate any data in this file that is sourced or attributed to a third party, it is your responsibility to determine whether permission is needed for that re-use and to obtain permission from the relevant owner.</p> <p>Attribution - Please cite the IEA's data as follows: International Energy Agency (2022), <i>Methane Tracker Database</i>, IEA, Paris. License: Creative Commons Attribution CC BY 4.0.</p> <p>Adaptations - If you create derived material based on IEA data, please use the following notice: Based on data from International Energy Agency (2022) <i>Methane Tracker Database - IEA</i>; as modified by [insert your legal entity name].</p>

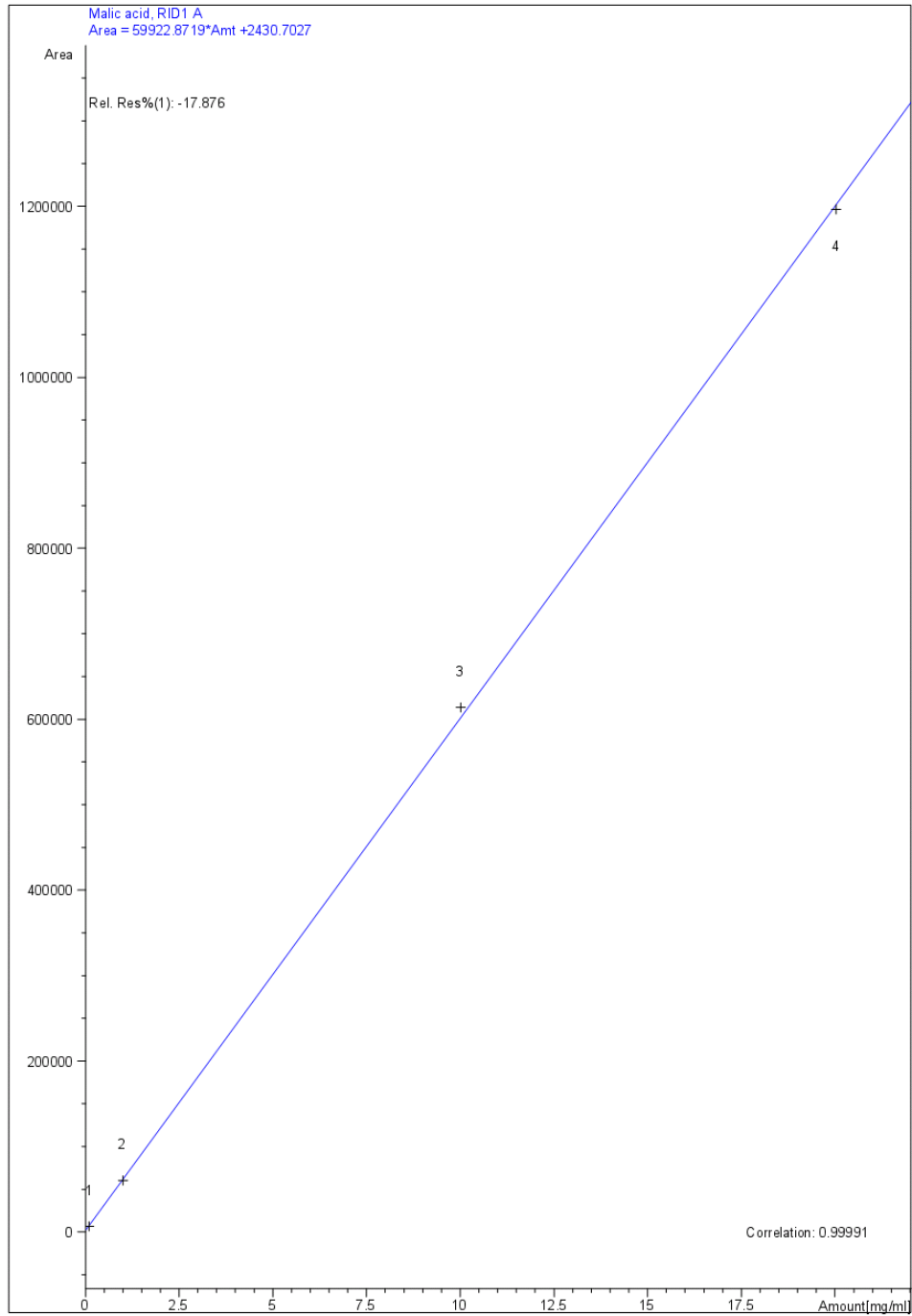
Appendix D

HPLC Standard Calibration Curves

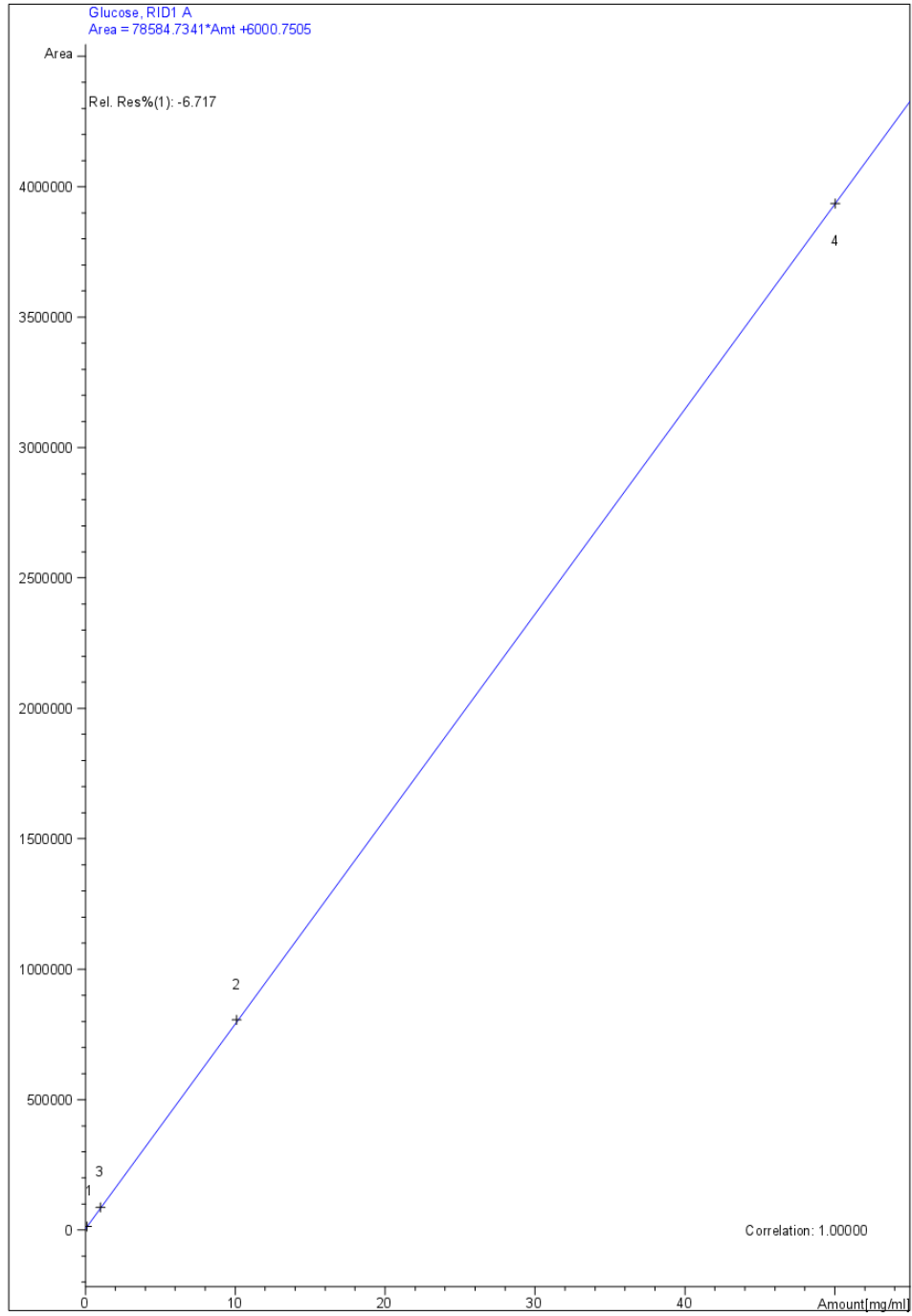
Calibration Curve



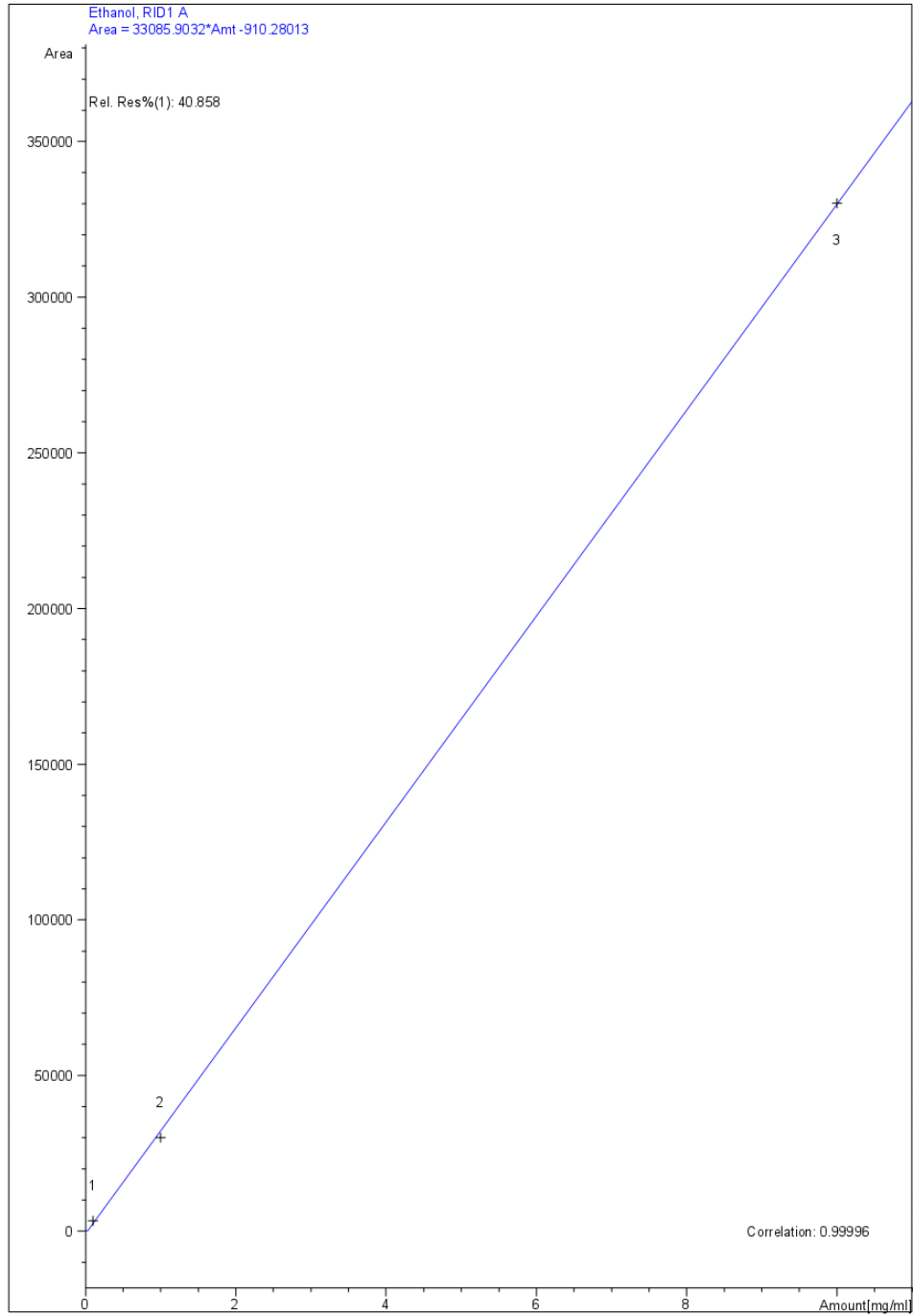
Calibration Curve



Calibration Curve



Calibration Curve



Calibration Curve

